Ge et al. Cell Communication and Signaling (2025) 23:420
https://doi.org/10.1186/s12964-025-02420-8

Cell Communication and Signaling

RESEARCH Open Access

BMAL1 modulation alleviates inflammatory responses in monocytes by targeting the Fis1-mediated mitochondrial unfolded protein response in high-altitude hypoxia

Yi-Ling Ge[1,2†], Jin Xu[1†], Yue Cai[3†], Bin Zhang[1], Si-Yuan He[1], Pei-Jie Li[1], Ying-Rui Bu[1], Lin Zhang[1], Zhi-Bin Yu[1], Heng Ma[4], Yong Liu[1*], Xiong-Wen Chen[5*] and Man-Jiang Xie[1*]

Abstract

Background Hypoxia-induced inflammation has been implicated in the progression of high-altitude illnesses. Mitochondria are key organelles for oxygen metabolism and inflammation that are controlled by circadian clocks. However, little is known regarding how circadian clocks sense hypoxic signals and trigger downstream mitochondrial responses.

Methods Human participants and mice were exposed to a real or simulated high-altitude setting of 5500 m. Multichannel fluorescence intravital microscopy was used for in vivo molecular imaging of inflammation. Bioinformatics analysis, myeloid-specific knockout mice, and RAW 264.7 cells were used to investigate the underlying inflammatory mechanisms.

Results We found that high-altitude hypoxia induced dynamic inflammatory activity in monocytes, characterized by significantly increased levels of cytokines (interleukin-6 [IL-6], IL-1β and monocyte chemoattractant protein-1) after acute (3-day) exposure, which returned to control levels after a prolonged (30-day) exposure. Bioinformatics analysis revealed that the core circadian transcription factor brain and muscle Arnt-like 1 (BMAL1) correlated positively with hypoxia-induced inflammation in monocytes. Mechanistically, BMAL1 induced NOD-like receptor protein 3 inflammasome activation in monocytes by targeting the Fis1-mediated mitochondrial unfolded protein response. Basic helix-loop-helix family member E40, a hypoxic stress-responsive transcription factor, directly promoted *Bmal1* transcription and triggered inflammation in monocytes. In contrast, myeloid-specific deletion of BMAL1 alleviated

†Yi-Ling Ge, Jin Xu and Yue Cai contributed equally to this work.

*Correspondence:
Yong Liu
liuyong@fmmu.edu.cn
Xiong-Wen Chen
xchen001@me.com
Man-Jiang Xie
xiemanjiang@fmmu.edu.cn

Full list of author information is available at the end of the article

the inflammatory activity of monocytes and circulating inflammation, both in vitro and in vivo, under high-altitude hypoxia.

Conclusions Our findings indicate that transcriptional activation of *Bmal1* in monocytes can potentially serve as a novel biomarker of hypoxia-induced inflammation. Our findings also suggest a novel approach for modulating the intrinsic clock, which might render organisms less vulnerable to high-altitude hypoxia.

Keywords High-altitude hypoxia, Inflammatory response, Mitochondrial unfolded protein response, BMAL1

Background

High-altitude regions are of great importance for travelling and economic activities [1], but people who ascend quickly without prior acclimatization are susceptible to several potentially lethal high-altitude illnesses [2, 3]. Acute mountain sickness (AMS) is the most prevalent condition associated with high-altitude regions and is characterized by nonspecific symptoms such as headache, lassitude, dizziness, and nausea. In some cases, AMS can progress to the more severe and fatal conditions, such as high-altitude cerebral edema and high-altitude pulmonary edema [2, 3]. Hypoxia-induced inflammatory responses are considered integral for progression of high-altitude illnesses [4, 5]. However, the specific cell types and mechanisms underlying high-altitude hypoxia are not fully understood.

Mitochondria are key organelles for sensing and metabolizing atmospheric oxygen. Recently, mitochondria have been shown to control inflammation [6]. Furthermore, many mitochondrial functions, such as oxidative metabolism, mitochondrial biogenesis, and mitochondrial dynamics, are controlled by circadian clocks [7–9]. As core regulators of gene transcription, the circadian clocks are endogenous timing systems that directly participate in many basic physiological and pathological processes [10, 11]. Hypoxia can induce internal circadian desynchronization of mitochondrial functions by disrupting the expression of clock genes in many hypoxic diseases such as ischemia, chronic obstructive pulmonary disease, and obstructive sleep apnea [12, 13]. Moreover, analysis of the Human whole blood transcriptome in highlanders at 5100m indicated that high-altitude hypoxia significantly affected daily variations in the expression of immunoregulatory genes [12, 14]. Recent evidence suggests that hypoxia resets circadian clocks. However, little is known about how circadian clocks sense hypoxic signals and trigger downstream inflammatory responses.

In this study, dynamic inflammatory responses were assessed in the circulating plasma and peripheral blood mononuclear cells (PBMCs) of human participants after acute (3-day) and prolonged (30-day) exposure to a high altitude of 5500 m. Bioinformatics analysis, myeloid-specific knockout mice, and RAW 264.7 cells were utilized to investigate the underlying mechanisms. We found that the core circadian transcription factor (TF) brain and muscle Arnt-like 1 (BMAL1) activated NOD-like receptor protein 3 (NLRP3) inflammasomes in monocytes by targeting the fission 1 (Fis1)-mediated mitochondrial unfolded protein response (UPR^{mt}). Furthermore, basic helix-loop-helix family member E40 (BHLHE40), a hypoxic stress-responsive transcription factor (TF), directly promoted *Bmal1* transcription and triggered an inflammatory response in monocytes. In contrast, myeloid-specific deletion of BMAL1 alleviated the inflammatory activity of monocytes and circulating inflammation in vitro and in vivo under high-altitude hypoxia. Our findings suggest a novel therapeutic approach for targeting the TF, BMAL1, in hypoxia-related diseases.

Methods

Human participants and study design

Twelve young, male lowlanders (aged 22–32 years) without a history of cardiorespiratory disease, severe mountain sickness, or recent exposure to altitudes > 2000 m were included in this before-and-after study. Human participants were transported by truck from the Kashgar region of China (1000 m above sea level) to the peak of Karakoram Mountain (5500 m above sea level). Venous blood (5 mL/person) was collected from 12 participants and PBMCs was collected from 6 participants at three different altitudes and time points: (1) before departure at an altitude of 1000 m, (2) on the third day at an altitude of 5500 m, and (3) on the 30th day at an altitude of 5500 m. To maintain consistency in terms of circadian rhythms, blood was collected at each altitude at 14:00.

The study protocol was approved by the Human Research Ethics Committee of the Air Force Medical University (AFMU) (approval number ChiCLR2000037401) and was conducted in accordance with the principles of the Declaration of Helsinki. All participants provided written informed consent to participate in the study after reading information about the study and explaining the procedures to them.

Mice

Global *Bmal1*-knockout mice (*Bmal1* $^{-/-}$ mice), *Bmal-1*$^{flox/flox}$ mice, and *Lyz2*-Cre mice were obtained Cyagen Biosciences (Shanghai, China) and had a C57BL/6 background. Wild-type (WT) C57BL/6 N mice were

purchased from the AFMU Animal Experimental Center. *Bmal1*$^{flox/flox}$ mice were crossed with *Lyz2*-Cre mice to selectively delete BMAL1 from myeloid cells throughout postnatal Life. The mice were housed under a 12-h light/12-h dark schedule with ad Libitum access to food and water. Male mice, aged 8–12 weeks, were used for the experiments. The animal study protocol was approved by the Animal Care and Use Committee of AFMU, protocol number 250,625. The study adhered to the guidelines set by the committee.

Cell culture

RAW 264.7 cells were obtained from Pricella Life Technology (Wuhan, China, catalog #CL-0190) and cultured in Dulbecco's modified Eagle's medium (DMEM) supplemented with 10% fetal bovine serum (Thermo Scientific, Rockford, IL, USA), 100 U/mL penicillin (Solarbio, Beijing, China), and 100 μg/mL streptomycin (Solarbio). Bone marrow-derived macrophages (BMDMs) were isolated from mouse tibias and femurs as described previously [15] and cultured for 7 days in Iscove's modified Dulbecco's medium supplemented with 10% fetal bovine serum (Thermo Scientific), penicillin–streptomycin (100 U/mL and 100 μg/mL, respectively; Sigma-Aldrich), and 10 ng/mL murine macrophage colony-stimulating factor (Peprotech, Wuhan, China). Human acute monocytic leukemia cell line THP-1 cells were obtained from National Collection of Authenticated Cell Cultures (Shanghai, China, catalog #SCSP-567) and cultured in RPMI 1640 medium supplemented with 10% fetal bovine serum (Thermo Scientific), 100 U/mL penicillin and 100 μg/mL streptomycin (Sigma-Aldrich), and 2 mM L-glutamine (Thermo Scientific).

Cultures were maintained under a Humidified atmosphere of 5% CO_2 and 95% air at 37 °C. For growth under hypoxic conditions, the cells were grown in a specialized humidified chamber (Heal Force, Shanghai, China) equilibrated with 1% oxygen, 94% nitrogen, 5% carbon dioxide for the indicated times.

Collecting plasma and PBMCs

Approximately 5 mL of human blood was collected using ethylenediaminetetraacetic acid as an anticoagulant for plasma extraction and then stored at −80 °C during transport until use. Following venous blood collection, PBMCs were immediately isolated from peripheral venous blood using a Peripheral Blood Mononuclear Cell Isolation Solution Kit (Solarbio, catalog #P6340) per the manufacturer's instructions.

RNA-sequencing analysis

Mouse PBMCs from control and high-altitude hypoxia groups were collected for RNA-sequencing analysis by Majorbio Biopharm Technology Co. (Shanghai, China), as described previously [16]. Transcript abundances were assessed using DESeq2, and genes with significant expression differences were identified using a fold-change threshold of ≥ 1.5. Kyoto Encyclopedia of Genes and Genomes (KEGG) and Gene Ontology (GO) enrichment analyses of differentially expressed genes (DEGs) were performed using Majorbio's website (www.majorbio.com).

Luminex liquid suspension chip detection

Luminex liquid suspension chip analysis was performed by Cloud-Clone Corp. (Wuhan, China), and a Human Magnetic Luminex Assay Kit (Cloud-Clone Corp.) was used to quantitate various factors in human plasma, per the manufacturer's instructions. Each human plasma sample was run on a single plate for each panel. We analyzed the inflammatory cytokines, interleukin-1β (IL-1β), interleukin-6 (IL-6), and monocyte chemoattractant protein-1 (MCP-1).

Assessing mitochondrial morphology and functions in cultured cells

We assessed the mitochondrial morphology, reactive oxygen species (ROS) levels, and mitochondrial membrane potentials (MMPs) of cultured cells (RAW264.6 cells and BMDMs) using the fluorogenic dyes, MitoTracker™ Red CMROS (Invitrogen by Thermo Fisher Scientific, Waltham, MA, USA, catalog #1800140), MitoSOX™ Red mitochondrial superoxide indicator (Invitrogen by Thermo Fisher Scientific, catalog #1842725), and MitoTracker™ Red CMROS (Invitrogen by Thermo Fisher Scientific, catalog #1800140), per the manufacturer's instructions. Images were acquired via the Operetta CLS high-content analysis system (Harmony, PerkinElmer, Germany) with a 63× water objective (1.15 numerical aperture). The fluorescence intensities of the images were evaluated via supervised machine learning using PhenoLOGIC Harmony 4.9 [17]. In the morphological analysis, the mitochondrial structure was isolated and analyzed from the microscopy images using Image J (NIH, Bethesda, MD, USA) to quantify the mitochondrial branch length, aspect ratio, and form factor values. The aspect ratio describes changes in mitochondrial length, while the form factor describes changes in both length and degree of branching. Mean values for the mitochondrial length, aspect ratio, and form factor were calculated from five randomly selected cells per experiment, with lower values representing increased mitochondrial debris.

Monocytes sorting from PBMCs

We sorted monocytes from PBMCs with a Pacific Blue-conjugated anti-mouse CD11b antibody (BioLegend, catalog #101223, 1:100 dilution) using flow-cytometry

sorting. For viability staining, propidium iodide (PI, BioLegend, catalog #421301, 1:50 dilution) was added before cell sorting, and monocytes were sorted as PI-CD11b+. FACSAria II (405 nm, 488 nm, 633 nm) with FACSDiva software v. 8.0.2 (BD Biosciences, San Jose, CA) was used for sorting.

Detecting mitochondrial functions and lymphocyte antigen 6 C (Ly6C)^{Hi} monocytes

Following monocytes sorting, we detected MMP, mitochondrial ROS, and Ly6C levels in monocytes with MitoTracker™ Red CMROS, MitoSOX™ Red mitochondrial superoxide indicator, and an APC-conjugated anti-mouse Ly6C antibody (BioLegend, catalog #128015, 1:300 dilution), per the manufacturers' instructions. Following staining, the MMP, mitochondrial ROS, and Ly6C^{Hi} levels in monocytes were assessed using NovoCyte 452,180,730,224 (ACEA Biosciences, San Diego, CA, USA).

Bioinformatics analysis

The gene-expression profiles of the GSE13510, GSE19994, and GSE196728 datasets were obtained from the Gene Expression Omnibus database. The data were processed using a robust multi-array average method for background correction, normalization, and expression calculations. Genes with an absolute $\log_2$ fold-change ($|\log_2 FC|$) of >1 and an adjusted p value of <0.05 were identified as DEGs using empirical Bayes analysis with the Limma package. GO and KEGG enrichment analyses of the DEGs were performed using the DAVID (Version 6.8) and Metascape (http://metascape.org/) databases. Data related to mitochondrial pathways were acquired from MitoCarta 3.0. The xCell algorithm was used to analyze 64 types of immune cells in human whole blood, employing histograms and box plots for visualization. The proportions of immune cells in each group were compared using the Wilcoxon rank–sum test.

Lentiviral transductions

Lentiviral vectors encoding a *Bmal1*-overexpression (pLV-hef1a-mNeongreen-P2A-Puro-WPRE-CMV-Arntl [NM_001368412, Mouse]–3flag) or empty control vector (pLV-hef1a-mNeongreen-P2A-Puro-WPRE-CMV-MCS-3flag) were designed and synthesized by SyngenTech (Beijing, China). RAW264.7 cells were seeded with complete growth medium (DMEM) supplemented with 10% fetal bovine serum, 100 U/mL penicillin and 100 μg/mL streptomycin), and incubated overnight at 37 °C in a 5% CO_2 atmosphere to achieve 30–50% confluency. Viral particles were diluted in complete medium to a final concentration of 1×10^8 transducing units/mL and then applied to the RAW264.7 cells for 24–48 h at 37 °C with 5% CO_2. For stable transduction, cells with stable bmal1 overexpression were selected based on puromycin resistance, and bmal1 overexpression was confirmed through western blot analysis.

Protein extraction and Western blot

Cells were dissociated with lysis buffer, followed by protein extraction, quantification, denaturation, and western blotting, as described [18]. The membranes were imaged using a Tanon 5200 luminous imaging system (Tanon, Shanghai, China). The antibodies used are Listed in Additional File 1: Table S1.

Measurement of mature IL-1β p17 and cleaved Caspase-1 p20

Culture medium from each well was mixed with double volumes of ice-cold acetone, vortexed, incubated at −20 °C overnight, and centrifuged at 12,000 × g at 4 °C for 10 min. The supernatants were removed, and the pellets were air-dried for 5 min at 50 °C. Then, 20 μL loading buffer was added to each sample, which was heated to boiling for 10 min before being subjected to SDS-PAGE and immunoblot analysis with antibodies against mature IL-1β (p17) and cleaved caspase-1 (p20). Adherent cells in each well were lysed with the lysis buffer described above, followed by immunoblot analysis to determine the content of various proteins in the cells.

RNA extraction and reverse transcription-quantitative polymerase chain reaction (RT-qPCR) analysis

Cells were homogenized using RNAiso (Takara, Otsu, Japan), and total RNA was extracted as described [18]. Complementary DNA was amplified using SYBR Premix Ex Taq (TaKaRa Bio). ACTB expression was detected as a control for quantification and normalization purposes. The data were analyzed using the relative Ct ($2^{-\Delta\Delta Ct}$) method. The sequences of the PCR primers used are Listed in Additional File 1: Table S2.

Chromatin Immunoprecipitation assay

Chromatin immunoprecipitation (ChIP) assays were performed using a ChIP Assay Kit (Thermo Fisher Scientific, catalog #26156). BMAL1-binding sites were amplified by PCR after immunoprecipitating DNA from sonicated cell lysates using a BMAL1 antibody. The sequences of the ChIP primers are presented in Additional File 1: Table S3.

Plasmid and oligonucleotide transfection

The GV141-*Bmal1* plasmid and small-interfering RNAs (siRNAs) targeting the *Bmal1* and *Bhlhe40* sequence (Genechem, Shanghai, China) were used. DNA plasmid and oligonucleotide transfection was performed using Lipofectamine3000 (Invitrogen, Carlsbad, CA, USA) and Opti-MEM Reduced-Serum medium (Invitrogen), as described previously [18]. The *Bmal1* siRNA sequence

was 5′-GCACGCGAUAGAUGGAAAGUUTT-3′. The *Bhlhe40* siRNA sequences were 5′-AGAACGUGUCAGC ACAATT-3′ (siRNA-1) and 5′-CCCUUCUCCUUUGGC ACA-UTT-3′ (siRNA-2).

Confocal fluorescence microscopy

The activation of inflammasome fluorescent-labeled ASC and NLRP3 was detected through fluorescence microscopy. HEK293T cells were transfected with ASC-RFP and NLRP3-GFP vectors, treated, and subsequently fixed with 4% paraformaldehyde and permeabilized with 1% Triton X-100. Nonspecific binding sites were blocked with 5% bovine serum albumin (BSA) and counterstained with DAPI to stain the nuclei. THP-1 cells were plated on poly-L-lysine-coated coverslips, and subsequently fixed, permeabilized, blocked, and incubated with anti-ASC antibody (Biodragon, BD-PT0365, 1:300 dilution) and Cy3- conjugated anti rabbit IgG (Abcam, ab6936, 1:1000 dilution), and counterstained with DAPI. Microscopic visual fields were captured randomly by a blinded experimenter using laser confocal microscopy (OLYMPUS, Tokyo, Japan).

Multichannel fluorescence intravital microscopy

To observe the migration and infiltration of monocytic cells into the vasculature under high-altitude hypoxia, we performed in vivo imaging of the mouse pulmonary vasculature and monocytic cells using an integrated multichannel fluorescence intravital microscopy (MFIM) imaging platform (IVIM-MS model, IVIM Technology). After a 3-day exposure to a simulated high-altitude of 5500 m, WT and myeloid-specific *Bmal1*-knockout (M-BKO) mice were injected with Evans blue angiography agent (Selleck, S4716, 30 μg/mg body weight per mouse) and an Alexa Fluor 488-conjugated anti-mouse CD11b antibody (BioLegend, catalog #101219, 2 μg in 150 μL saline per mouse) through the tail vein. The mice were then intubated via the trachea, and the chest skin, pleura, and ribs were sequentially incised to expose the peripheral Lungs for imaging. Three mice were used from each group, and the pulmonary vasculature was observed at multiple time points. Representative images and videos were acquired, and cells were quantified using Image J. Cells were considered adherent if they remained stationary on the vasculature for more than 10 s. Vessel diameter was measured using Image J to normalize the number of adherent cells.

Statistical analysis

All the quantitative data are presented as the mean ± the standard error of the mean (SEM). Comparisons between two groups were performed using two-tailed unpaired or paired Student's t-tests. Differences among multiple groups were assessed using one-way analysis of variance (ANOVA), followed by Bonferroni's post-hoc correction. Statistical analyses were performed using GraphPad Prism software (version 9.0; Nashville, TN, USA), and differences were considered statistically significant at $P < 0.05$ [19].

Results

PBMCs were sensitive to acute high-altitude hypoxia and contributed to systemic circulating inflammation

To detect dynamic changes in the inflammatory response under high-altitude hypoxia, a human study was conducted using 12 male volunteers. These participants were transported by truck to climb the top of Karakoram Mountain (5500 m), and peripheral blood samples (5 mL/person) were collected at three different time points. As a baseline reference, the first blood sample was collected before departure, at an altitude of 1000 m. The second blood collection was performed on day 3 at 5500 m on Karakoram Mountain, and the third collection was completed on day 30 at 5500 m (Fig. 1A).

The proinflammatory cytokines IL-1β and IL-6 and the chemokine MCP-1 are three master cytokines that are generally recognized as links between high-altitude hypoxia and inflammatory responses [4, 20, 21]. In this study, the plasma levels of these three inflammatory cytokines were measured in Luminex assays. The results indicated that the plasma levels of inflammatory cytokines were significantly higher on day 3 at 5500 m than at the baseline (1000 m) but that were decreased by day 30 at 5500 m (Fig. 1B; Additional File 1: Table S4). These data suggest that acute (3-day) high-altitude hypoxia triggered systemic inflammation, which gradually decreased during the continuous (30-day) exposure.

Inflammatory cytokines are produced and secreted by multiple cells. To identify the specific source of circulating cytokines in response to high-altitude hypoxia, we performed xCell analysis to measure the abundances of 64 immune-related cell types within human whole blood based on GSE196728. Monocytes and macrophages showed significantly higher abundances in the high-altitude group (La Rinconada, Peru, 5,100 m) than in the sea-level group (Additional File 1: Figure S1).

Next, monocyte-enriched PBMCs were isolated from the human participants ($n = 6$) while climbing to higher altitudes and analyzed by RT-qPCR to detect the mRNA-expression levels of different inflammatory cytokines including IL-6, IL-1β and C-C motif chemokine receptor 2 (CCR2, the receptor for MCP-1). Inflammatory cytokine expression was significantly higher on day 3 at 5500 m, although it had decreased by day 30 (Fig. 1C). Spearman and Pearson correlation analyses suggested that increased mRNA-expression levels of inflammatory cytokines in human PBMCs correlated significantly and positively with increased protein levels of the corresponding

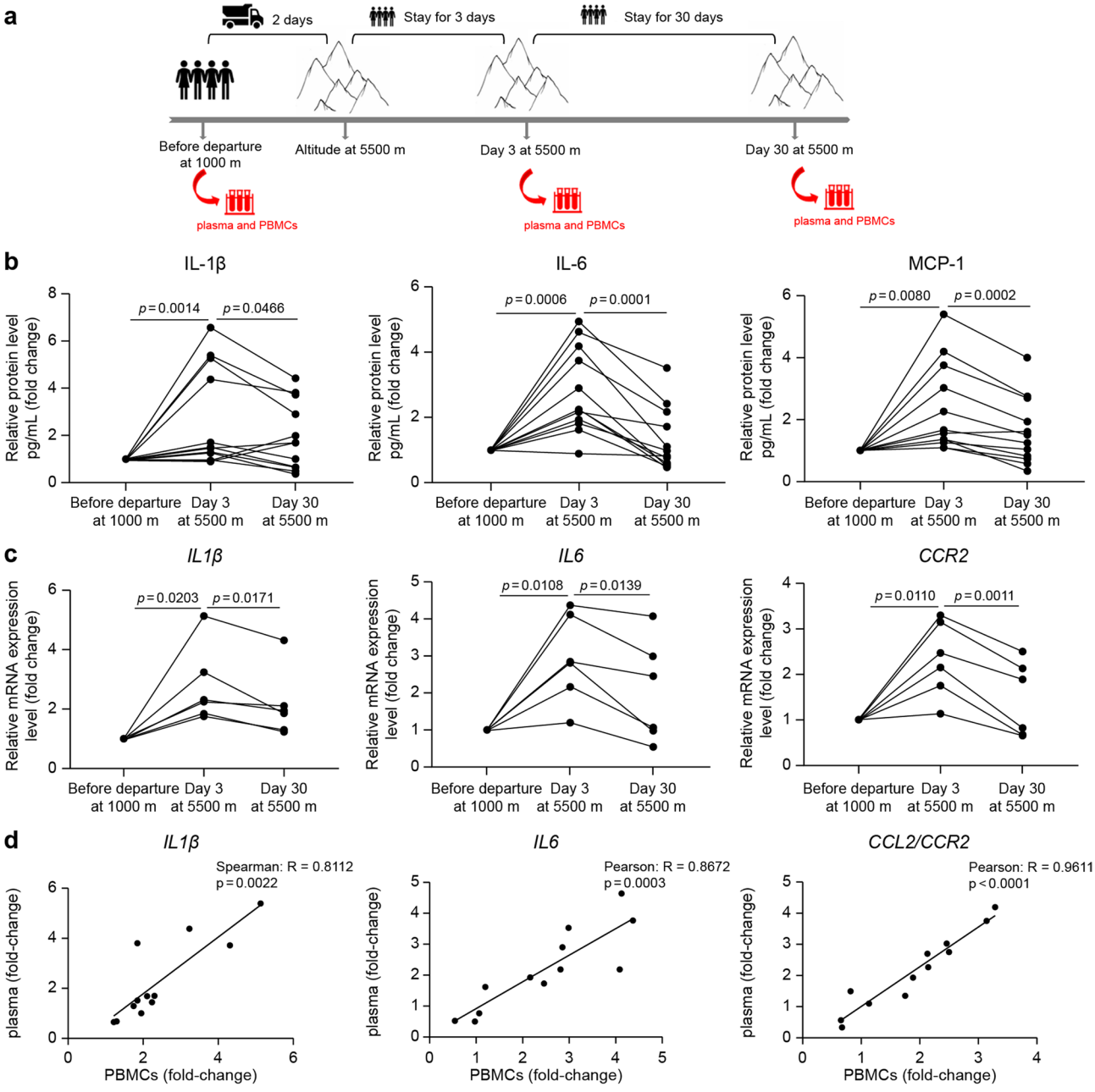

Fig. 1 Expression changes of inflammatory cytokines (IL-1β, IL-6, and MCP-1) in human plasma and PBMCs. Inflammatory cytokine levels significantly increased after acute (3-day) high-altitude hypoxia and returned to control levels after prolonged (30-day) exposure. **A–D** Human participants were driven to the Karakoram Mountain (~5500 m) by truck and stayed for 30 days. Human plasma and PBMCs were collected at on days 3 and 30 at Karakoram Mountain (~5500 m) and before departure from the Kashgar region (~1000 m) as a baseline reference. Flow diagram of the human study (**A**). The protein-expression levels of IL-1β, IL-6, and MCP-1 in human plasma were measured in Luminex assays conducted for the indicated time points ($n = 12$, **B**). IL-1β, IL-6, and CCR2 mRNA expression in human PBMCs were investigated by RT-qPCR for each time point ($n = 6$, **C**). Spearman and Pearson correlation analyses were used to investigate correlations between inflammatory cytokines in human plasma and those in human PBMCs (**D**). Statistical significance was determined using a paired Student's two-tailed t test (**B**, **C**)

inflammatory cytokines in human plasma during altitude climbing (Fig. 1D). These results indicate that the inflammatory activities of monocyte-enriched PBMCs became activated under acute high-altitude hypoxia and contributed to systemic inflammation.

M-BKO mice showed significantly lower monocyte inflammatory activity and systemic circulating inflammation under acute high-altitude hypoxia

High-altitude hypoxia is usually accompanied by circadian dyssynchrony, which may exacerbate inflammatory pathologies [14]. In this study, bioinformatics

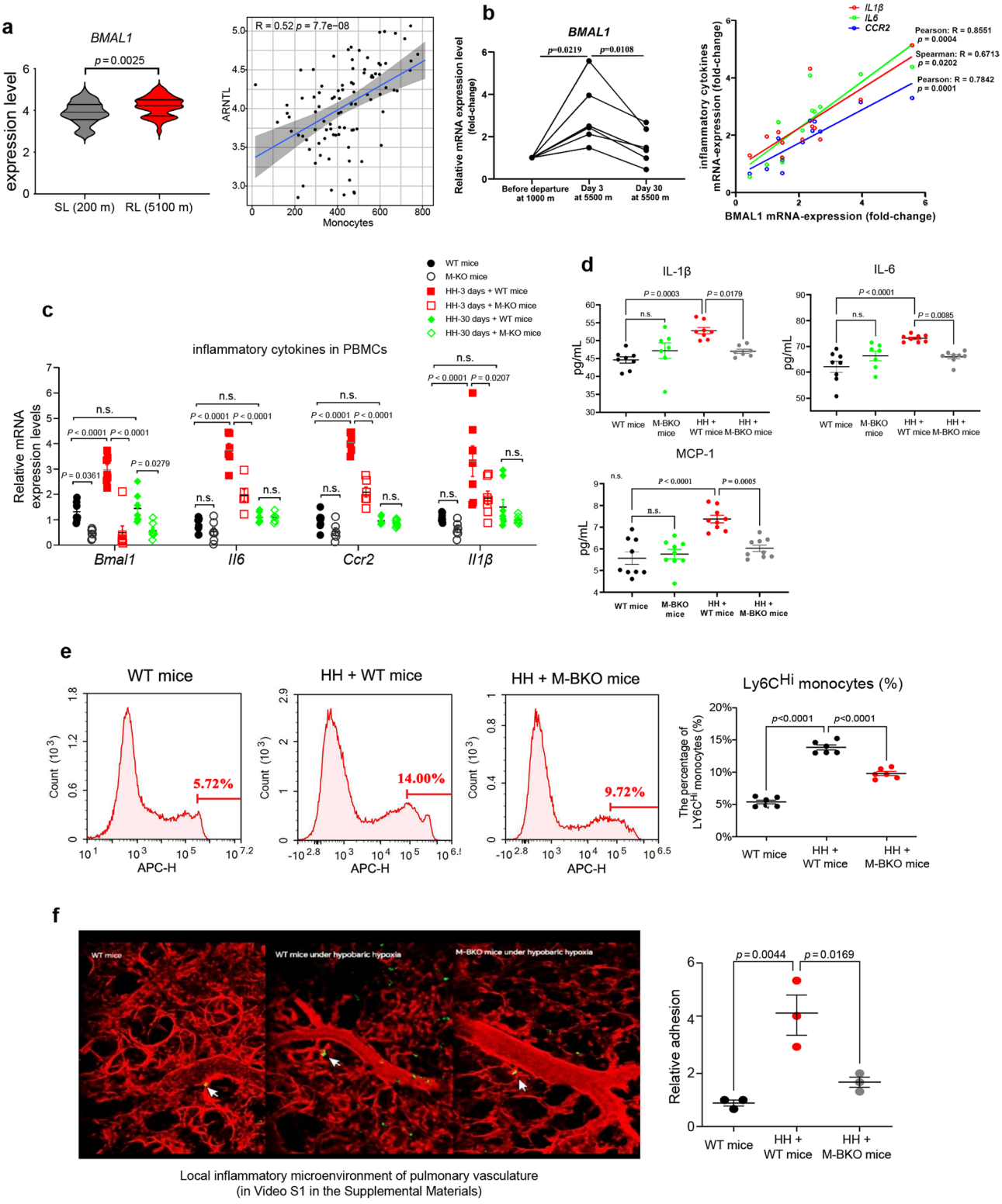

Fig. 2 (See legend on next page.)

(See figure on previous page.)

Fig. 2 Association of *Bmal1* expression with inflammation in human PBMCs and M-BKO mice. *Bmal1* expression significantly promoted monocyte inflammatory activity and M-BKO mice showed significantly lower circulating inflammation after a 3-day exposure to high-altitude hypoxia. **A** Spearman correlation analysis was used to investigate the correlation between *Bmal1* expression (left) and monocyte abundance (right) in human whole blood at a high altitude (5100 m). Source data were obtained from the GSE196728 dataset. **B***BMAL1* mRNA expression in human PBMCs at three time points (before departure and on days 3 and 30 at 5500 m) were detected by RT-qPCR analysis ($n=6$, left). Spearman and Pearson correlation analyses were performed to investigate correlations between *BMAL1* mRNA expression and *IL1β*, *IL6*, and *CCR2* mRNA expression in human PBMCs (right). **C** WT and M-BKO mice were exposed to a simulated high-altitude condition (5500 m) for 0, 3, or 30 days. RT-qPCR analysis revealed the mRNA expression of *Il6*, *Il1β*, and *Ccr2* in mouse PBMCs ($n=6$–8). **D–F** WT and M-BKO mice were exposed to a simulated 5500 m for 0 or 3 days. ELISA analysis was performed to detect IL-6, IL-1β, and MCP-1 protein expression in mouse plasma ($n=6$–8, **D**); flow cytometric analysis detected the inflammatory ($Ly6C^{Hi}$) monocyte ratios in mouse PBMCs ($n=6$, **E**). Monocytes sorting strategy was shown in Additional File 1: Figure S3; MFIM was used to detect in vivo adherent inflammatory cells (green) in the pulmonary vasculature (red) ($n=3$, **F**,Video S1). The data shown represent the mean ± SEM **(C–F)**. Statistical significances were determined by performing an unpaired Student's 2-tailed t test with Welch's correction (**A**), a paired Student's two-tailed t test (**B**), or 1-way ANOVA followed with Tukey's multiple-comparisons test (**C–F**).

analysis of human whole blood at high altitudes (based on GSE196728) indicated that the increased abundance of monocytes at high altitudes correlated positively with activation of the circadian gene, *Bmal1* (Fig. 2A). Next, *Bmal1* mRNA expression was detected in Human PBMCs at 5500m, and the results suggested that *Bmal1* mRNA expression significantly increased by day 3 at 5500 m but was lower on day 30 (Fig. 2B). Spearman and Pearson correlation analyses showed *Bmal1* mRNA expression correlated significantly and positively with *IL6*, *IL1β*, and *CCR2* expression in human PBMCs during the process of altitude climbing (Fig. 2B). The mRNA expression of additional clock genes, including *Per2*, *Nr1d1*, *Clock*, and *Cry1*, was analyzed in PBMCs isolated from mice exposed to a simulated altitude of 5500 m for 3 or 30 days. The results showed that *Per2* mRNA expression significantly increased on day 3 compared with that in the control group but did not significantly change on day 30, which was consistent with *Bmal1* mRNA expression. In contrast, *Clock* mRNA expression was significantly upregulated on day 30 but unaltered on day 3 at 5500 m (Additional File 1: Figure S2).

To investigate the effect of *Bmal1* expression on monocytes, M-BKO mice were generated and exposed to a simulated altitude of 5500 m for 3 or 30 days in a high-altitude chamber. RT-qPCR and flow cytometric analyses showed the mRNA-expression levels of inflammatory cytokines (*Il1β*, *Il6*, and *Ccr2*) (Fig. 2C) and the inflammatory ($Ly6C^{Hi}$) monocyte ratio (Fig. 2E and Additional File 1: Figure S3) in mouse PBMCs under acute high-altitude hypoxia were significantly lower in M-BKO mice than in WT mice. Enzyme-linked immunosorbent assay (ELISA) analysis showed the plasma levels of IL-6, MCP-1, and IL-1β also were significantly lower in the M-BKO mice (Fig. 2D).

Next, WT and M-BKO mice were injected with a low concentration of a $CD11b^{+}$ fluorescent antibody to label monocytic cells in vivo, and the infiltration of and interactions between monocytic cells and the pulmonary vasculature were visualized in real time with MFIM. Exposure to acute high-altitude hypoxia clearly induced monocytic cell adhesion and infiltration into the pulmonary vasculature, which was significantly lower in M-BKO mice than in WT mice (Fig. 2F and Additional File 2: Video S1). These data indicate that, under acute high-altitude hypoxia, transcriptional *Bmal1* activation in monocytes was crucial for their inflammatory activity and that myeloid-specific *Bmal1* knockout significantly alleviated the inflammatory activity of monocytes and systemic circulating inflammation.

High-altitude hypoxia induced the UPR^{mt} in monocytes under acute high-altitude hypoxia

To identify potential inflammatory signals occurring in response to acute high-altitude hypoxia in monocytes, RNA-sequencing analysis was conducted using PBMCs from mice exposed to a simulated altitude of 5500 m for 3 days in a high-altitude chamber (Additional File 1: Figure S3A). GO enrichment analysis revealed many DEGs that were enriched for mitochondrion-related terms (Fig. 3A). We identified 96 mitochondrial DEGs through intersection analysis with the Mitocarta 3.0 database (an inventory of mammalian mitochondrial proteins and pathways) (Additional File 1: Figure S3B and Table S5), and GO enrichment analysis revealed that these mitochondrial DEGs were mainly enriched for terms related to mitochondrial protein homeostasis (red fonts), suggesting the potential involvement of mitochondrial protein stress signaling (Fig. 3B).

The UPR^{mt} is a specific mitochondrial stress response activated by mitochondrial protein disturbances [22]. UPR^{mt} markers (lon peptidase 1 [LONP1], AFG3-like AAA ATPase 2 [AFG3L2], and heat shock protein 60 [HSP60]) were detected in human PBMCs via RT-qPCR analysis during the process of altitude climbing. The UPR^{mt} was significantly activated by day 3 at 5500 m but was significantly lower on day 30 (Fig. 3C).

Mice were placed in a high-altitude chamber at a simulated altitude of 5500 m for 3, 7, or 30 days. The mRNA-expression levels of UPR^{mt}-marker genes (*Lonp1*, *Afg3l2*, and *Hsp60*) in mouse PBMCs were investigated by RT-qPCR analysis. The results showed that UPR^{mt}-marker gene-expression levels were significantly higher on day 3

than in the control group but that no significant alterations were detectable on days 7 and 30 (Fig. 3D).

Flow cytometric analysis showed that mitochondrial ROS (mtROS) levels increased in monocytes and that MMPs decreased significantly after simulated exposure to 5500 m for 3 days (Fig. 3E, F and Additional File 1: Figure S3). These data indicate that mitochondrial stress of UPR^{mt} activation was triggered and involved in monocyte inflammatory responses under acute high-altitude hypoxia.

Transcriptional activation of Bmal1 drove UPR^{mt} and induced NLRP3 inflammasome activation in monocytes under hypoxia

Mitochondrial function and homeostasis are regulated by circadian clocks [23–25], and the circadian gene *Bmal1* promoted systemic inflammation and mortality in septic mice by disrupting mitochondrial homeostasis in monocytes [26]. In this study, *Bmal1* function was investigated after overexpressing it in RAW264.7 cells via lentivirus transduction (Fig. 4B–C) or by deleting it in BMDMs ($Bmal1^{-/-}$ BMDMs), which were isolated from global *Bmal1*-knockout mice (Fig. 4E–H). Western blot analyses showed that the protein levels of UPR^{mt} markers (ATF4, ATF5, p-EIF2A/EIF2A, LONP1, AFG3L2, and HSP60) were significantly higher in RAW264.7 cells overexpressing BMAL1 (High-BMAL1 cells), under both normoxic and 1% oxygen hypoxic conditions (Fig. 4B). In contrast, *Bmal1* deletion alleviated hypoxia-induced oxidative stress by decreasing mtROS levels and increasing the MMP (Fig. 4E) and markedly attenuated UPR^{mt} activation in the BMDMs under 1% oxygen hypoxic conditions (Fig. 4F).

Many mitochondria-dependent molecules cross-talk with NLRP3 inflammasome signaling and thereby activate inflammatory responses [23–25, 27, 28]. In the present study, we observed that *NLRP3* and *IL1β* mRNA expression levels in human and mouse PBMCs were significantly elevated on day 3 after exposure to an altitude of 5500 m, but gradually decreased by days 7 and 30 (Additional File 1: Figure S4). To investigate the role of the *Bmal1*-UPR^{mt} pathway in NLRP3 inflammasome signaling, HEK293T cells co-transfected with ASC-RFP and NLRP3-GFP constructs were subsequently transfected with either *Bmal1* siRNA or *Bmal1* overexpression vector and then treated with 60 μg/mL doxycycline, an antibiotic that inhibits the translation of mitochondrial-encoded proteins to create protein disequilibrium and induce UPR^{mt}. The activation of NLRP3 inflammasome signaling was assessed via confocal microscopy by detecting the formation of ASC oligomeric specks and their co-localization within NLRP3. Following treatment with doxycycline for 48 h, ASC oligomeric specks were formed and co-localized with NLRP3 in HEK293T cells, and *Bmal1* overexpression significantly enhanced while *Bmal1* knockdown attenuated the activation of inflammasome signaling in the context of mitochondrial stress (Fig. 4A).

Western blot analyses showed that NLRP3 inflammasome signaling (NLRP3, cleaved Caspase-1 p20/pro-Caspase-1) and inflammatory cytokines (CCR2, IL-6 and IL-1β p17/pro- IL-1β) were significantly elevated in High-Bmal1 RAW264.7 cells under both normoxic and 1% oxygen hypoxic conditions (Fig. 4C and D). However, the activation of NLRP3 inflammasome signaling and inflammatory cytokines under hypoxic condition was significantly alleviated in *Bmal1*-deficient BMDMs (Fig. 4G and H). Similarly, in human monocytic THP-1 cells, the signaling pathway of UPR^{mt}/NLRP3 inflammasome/inflammatory cytokines was also significantly upregulated by *Bmal1* overexpression but inhibited by *Bmal1* knockdown under both normoxic and 1% oxygen hypoxic conditions (Additional File 1: Figure S5). These results indicate that the transcriptional activation of *Bmal1* under hypoxia promoted monocyte inflammatory responses by activating UPR^{mt} and NLRP3 inflammasome signaling.

BMAL1 modulated the UPR^{mt} and mito-inflammation in monocytes by promoting Fis1-mediated mitochondrial fission under hypoxia

Under environmental stress, mitochondrial fission and fusion are important mitochondrial quality-control mechanisms that help maintain mitochondrial protein homeostasis. With PBMCs from mice exposed to a simulated altitude of 5500 m for 3 days, GO enrichment analysis revealed that some mitochondrial DEGs were also enriched in terms of the mitochondrial fission-related pathway (Fig. 3B, blue font). RT-qPCR analysis revealed that the mRNA-expression levels of *Bmal1* and mitochondrial fission genes (*Fis1* and dynamin-related protein 1 [*Drp1*]) were significantly higher in mouse PBMCs under acute high-altitude hypoxia, while those of mitochondrial fusion genes (mitofusin 1 [*Mfn1*], *Mfn2*, and optic atrophy 1 [*Opa1*]) were significantly lower (Fig. 5A).

Next, DNA fragments bound to the BMAL1 protein in RAW264.7 cells were recovered by performing ChIP assays. Reverse transcriptase-polymerase chain reaction (RT-PCR) and RT-qPCR analyses of the ChIP products indicated that BMAL1 bound to the promoter region of *Fis1* and stimulated its transcription in mouse monocytes (Fig. 5B). Overexpressing *Bmal1* in RAW264.7 cells significantly increased FIS1 protein expression under both normoxic and hypoxic conditions (Fig. 5C), and deleting *Bmal1* ($Bmal1^{-/-}$) significantly decreased *Fis1* mRNA (Fig. 5D) and protein (Fig. 5E) expression, confirming the important role of BMAL1 in promoting *Fis1* transcription.

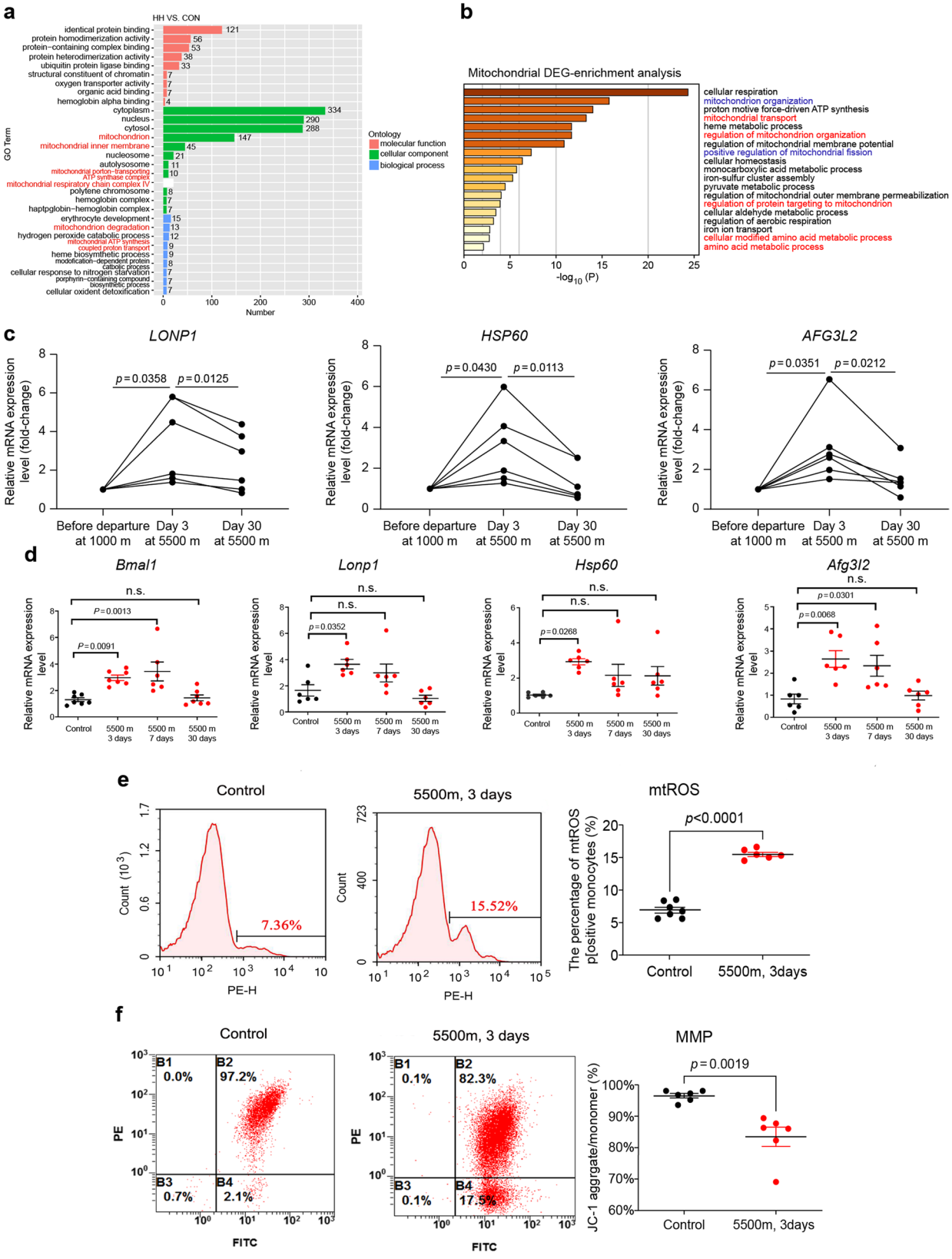

Fig. 3 (See legend on next page.)

(See figure on previous page.)

Fig. 3 UPR^{mt} was activated in monocytes during a 3-day exposure to high-altitude hypoxia. **A**, **B** Mice were exposed to a simulated altitude of 5500 m for 3 days. PBMCs isolated from control and high-altitude hypoxic mouse groups were subjected to RNA-sequencing analysis ($n = 5$). The 30 most significant GO terms based on DEG enrichment analysis between the control and high-altitude hypoxia groups (mitochondria-related pathways marked with red font, **A**). Mitochondrial DEGs were further subjected to GO enrichment analysis; the pathways involved in mitochondrial protein homeostasis are indicated with red font, and pathways involved in mitochondrial fission are indicated with blue font (**B**). **C**, **D** RT-qPCR analysis was performed to investigate mRNA-expression levels of UPR^{mt} markers (*LONP1*, *HSP60*, and *AFG3L2*) in human PBMCs at three time points (before departure and after 3 or 30 days at 5500 m) (**C**) and in PBMCs from mice subjected to a simulated altitude of 5500 m for 3, 7, or 30 days (**D**). **E**, **F** Flow cytometric analysis was performed to quantify mitochondrial ROS (**E**) and MMPs (**F**) in circulating monocytes from mice subjected to a simulated altitude of 5500 m for 3 days ($n = 6$). Monocytes sorting strategy was shown in Additional File 1: Figure S3. The data shown represent the mean ± SEM (**D–F**). Statistical significance was determined by performing a paired Student's two-tailed t test (**C**), 1-way ANOVA followed by Tukey's multiple-comparisons test (**D**), or an unpaired Student's two-tailed t test with Welch's correction (**E**, **F**)

To study the regulatory role of BMAL1 in the mitochondrial morphology (fission and fusion), WT and Bmal1$^{-/-}$ BMDMs were stained with Mito-Tracker and cultured under 1% oxygen hypoxia for 24 h. An abundance of punctate mitochondria with a loss of filamentous cells was observed in WT BMDMs under hypoxia; however, Bmal1$^{-/-}$ BMDMs exposed to showed mostly rod-like mitochondria (Fig. 5F). Consistently, western blot analysis indicated that mitochondrial fission proteins (DRP1 and FIS1) were significantly upregulated, whereas mitochondrial fusion proteins (OPA1, MFN1, and MFN2) were significantly downregulated in WT BMDMs under hypoxia; however, the opposite results were observed with Bmal1$^{-/-}$ BMDMs under hypoxia (Fig. 5G). These findings suggest that transcriptional *Bmal1* activation targeted *Fis1* to promote mitochondrial fission in monocytes under hypoxia.

To investigate the role of mitochondrial fission in hypoxia-induced mito-inflammation in monocytes, we treated them with mitochondrial division inhibitor-1 (Mdivi-1), which inhibited mitochondrial fission in dose- and time-dependent manners (Fig. 6A). Inhibiting mitochondrial fission with 50 μM Mdivi-1 markedly alleviated *Bmal1* overexpression-induced mitochondrial dysfunctions, such as decreased MMP levels and mitochondrial ROS production, as well as UPR^{mt}, NLRP3 inflammasome, and inflammatory response activation in RAW264.7 cells under both normoxic and hypoxic conditions (Figs. 6B and 7D). These results suggest that hypoxia-induced *Bmal1* overexpression triggered mitochondrial stress and activated mito-inflammatory signaling by promoting Fis1-mediated mitochondrial fission in monocytes.

TF, BHLHE40, stimulated Bmal1 transcription in monocytes under hypoxia

Above, we demonstrated that *Bmal1* transcriptional activation drove the initiation of mitochondrial stress and inflammatory responses in monocytes under high-altitude hypoxia; however, few reports have described factors that can trigger *Bmal1* transcription. TFs and histone modifications represent two important mechanisms accounting for the activation of gene transcription as previously reported [29]. Hence, in this study, we conducted a set of bioinformatic analyses to identify TFs or histone modifications that could account for the transcriptional activation of *Bmal1* in monocytes under hypoxia (Fig. 7A). We used the JASPAR database to identify 68 upstream TFs that can potentially bind promoter and regulatory sites in the *Bmal1* gene (Table 1). The intersection of the mRNA-expression profiles of peripheral human leukocytes and THP-1 monocytes (GSE135109 and GSE199947, respectively) revealed 16 common DEGs that arose in monocytes in response to hypoxia (Additional File 1: Figure S6A, S6B and Table S6; Fig. 7B), which were enriched for regulation of DNA-binding TF activity pathway (Fig. 7C).

Through ingenuity pathway analysis and the intersection with these 16 common DEGs, the basic helix-loop-helix family member E40 (BHLHE40) was identified from 234 candidate factors (Additional File 1: Table S7) that regulate the 68 upstream TFs of *Bmal1* (Table 1; Additional File 1: Figure S6C; Fig. 7D). BHLHE40 is an immediate–early response gene in macrophages that has been reported to function as a hypoxia-inducible factor (HIF)–1a-targeting TF (Additional File 1: Figure S7). Here, *Bhlhe40* mRNA expression increased significantly in mouse PBMCs (Fig. 7E) and RAW264.7 cells (Fig. 7G) under hypoxia. Transfection with *Bhlhe40* siRNAs significantly decreased *Bmal1* mRNA expression (Fig. 7F and G) and alleviated the hypoxia-induced UPR^{mt} (Fig. 7H) and inflammatory response (Fig. 7I) in RAW264.7 cells. Overexpressing *Bmal1* in RAW264.7 cells did not affect *Bhlhe40* mRNA expression, although it significantly blocked the inhibitory effect of *Bhlhe40* siRNAs in terms of UPR^{mt} and inflammatory response activation (Fig. 7G-7I). These results suggest that BHLHE40 functioned as an upstream signaling molecule involved in *Bmal1* transcriptional activation that elicited mito-inflammatory signaling in monocytes under hypoxia.

Using ChIPBase v3.0 (https://rnasysu.com/chipbase3/index.php), we predicted 29 histone modifications involved in regulating *Bmal1* transcription (Table 2). The lysine demethylase 5 (KDM5) family of histone demethylases comprises oxygen-dependent dioxygenases that target changes in histone 3 lysine 4 (H3K4) methylation

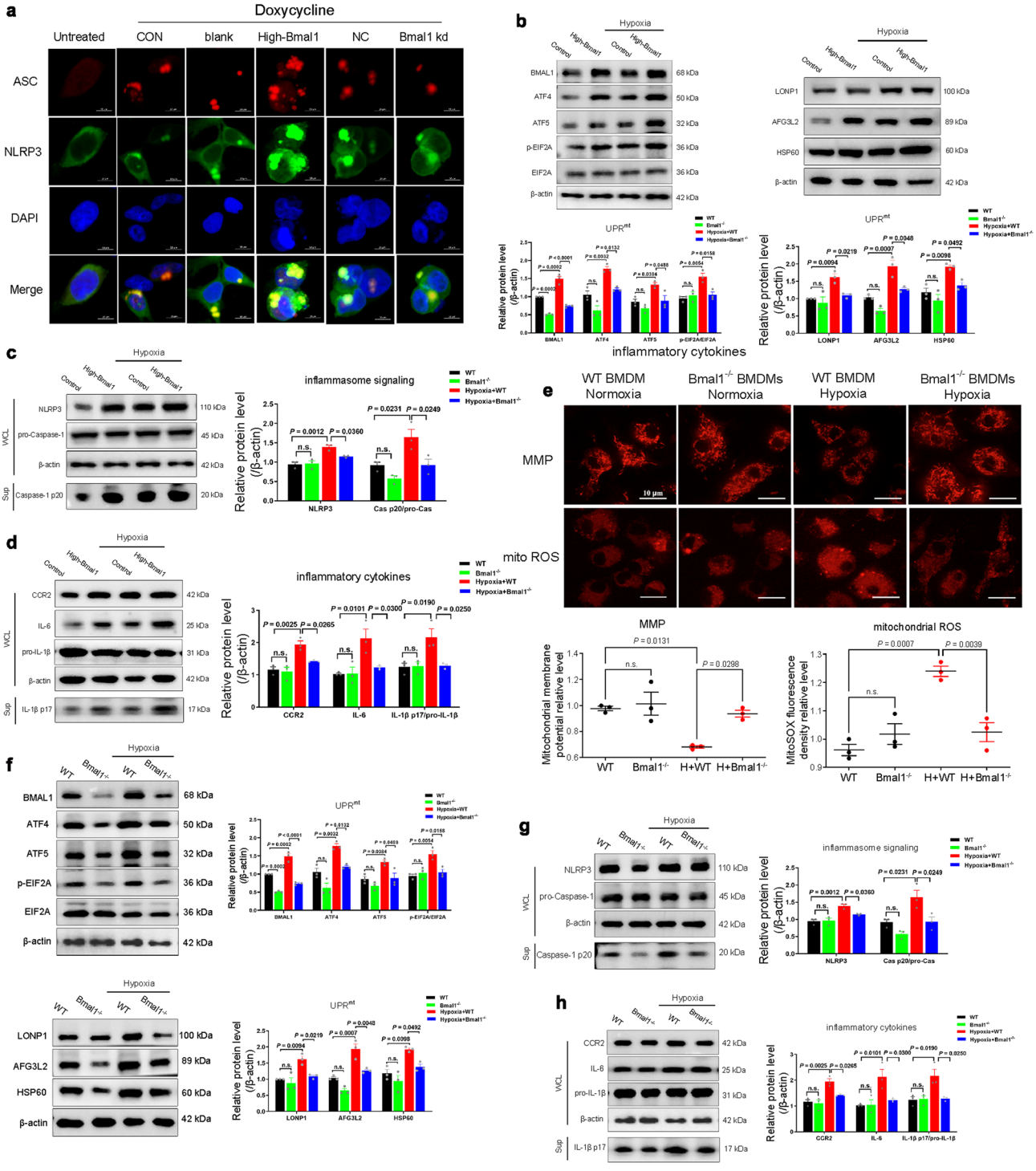

Fig. 4 (See legend on next page.)

(See figure on previous page.)

Fig. 4 Transcriptional activation of *Bmal1* induced the UPR^{mt} and NLRP3 inflammasome activation in monocytes under hypoxia. **A** HEK293T cells were co-transfected with ASC-RFP vector/NLRP3-GFP vector, and either ASC-RFP vector/NLRP3-GFP vector/*Bmal1*siRNA or ASC-RFP vector/NLRP3-GFP vector/*Bmal1* overexpression vector were treated with a mitochondrial stress inducer (doxycycline, 60 μg/mL) for 48 h. Confocal microscopy of inflammasome fluorescent-labeled for ASC (red) and NLRP3 (green). Scale bars = 10 μm. **B–D** RAW264.7 cells were transduced with a lentivirus to generate stable *Bmal1*-overexpressing mouse monocytes, which were cultured with 21% oxygen (normal condition) or 1% oxygen (hypoxic condition) for 24 h. Western blot analysis was performed to investigate the protein-expression levels of UPR^{mt} markers (ATF4, ATF5, p-EIF2A/EIF2A, LONP1, HSP60, and AFG3L2, **B**), NLRP3 inflammasome signaling (NLRP3, Caspase-1 p20/pro-Caspase-1, **C**), and inflammatory cytokines (CCR2, IL-6 and IL-1β p17/pro-IL-1β, **D**) in RAW264.6 cells ($n = 3$). **E–H** Bmal1$^{-/-}$ and WT BMDMs were isolated from global *Bmal1*-knockout mice and WT mice, respectively, and cultured under 21% or 1% oxygen for 24 h. Fluorescent probe staining quantified MMP (left) and mitochondrial ROS (right) levels in BMDMs ($n = 3$, scale bars = 20 μm, **E**). Western blot analysis showed the protein levels of UPR^{mt} markers (ATF4, ATF5, p-EIF2A/EIF2A, LONP1, HSP60, and AFG3L2, **F**), NLRP3 inflammasome-signaling markers (NLRP3, Caspase-1 p20/pro-Caspase-1, **G**), and inflammatory cytokines (CCR2, IL-6, and IL-1β p17/pro-IL-1β, **H**) in BMDMs ($n = 3$). The data shown represent the mean ± SEM. Statistical significance was determined by performing 1-way ANOVA followed by Tukey's multiple-comparisons test (**B–H**). Abbreviation: NC, negative control; kd, knockdown; WCL, whole cell lysate; Sup, supernatant

(me1, me2, and me3) to regulate gene expression under hypoxic conditions. In this study, we confirmed that hypoxia significantly increased the protein levels of H34Kme3 in PBMCs from mice subjected to a simulated altitude of 5500 m for 3 days (Fig. 8A) and in RAW264.7 cells cultured under 1% oxygen hypoxic conditions for 12–24 h (Fig. 8B). However, inhibiting KDM5 demethylases by treating cells with CPI-455 (a KDM5 demethylase-family inhibitor) (Fig. 8C) or by transfecting cells with siRNAs against *Kdm5a* (Fig. 8D) and *Kdm5c* (Fig. 8E) did not significantly affect *Bmal1* mRNA expression, excluding the potential role of KDM5 demethylase-mediated H3K4me1/2/3 in activating *Bmal1* transcription under hypoxia.

Discussion

The major and novel findings of this study are as follows: (1) High-altitude hypoxia induced dynamic inflammatory activity in monocytes characterized by significantly increased levels of cytokines after an acute (3-day) exposure, which returned to baseline levels after a prolonged (30-day) exposure. (2) The core circadian TF BMAL1 induced NLRP3 inflammasome activation in monocytes by targeting Fis1-mediated UPR^{mt}. (3) BHLHE40, a hypoxic stress-responsive TF, directly promoted *Bmal1* transcription and triggered inflammatory responses in monocytes. (4) Myeloid-specific deletion of BMAL1 alleviated the inflammatory activity of monocytes and circulating inflammation in vitro and in vivo under high-altitude hypoxia.

High-altitude hypoxia induced a dynamic inflammatory response in humans and M-BKO mice showed significantly attenuated inflammatory responses

Inflammation plays a key role in the physiological response to hypoxic stress, where the production of several inflammatory mediators could signal tissue damage and initiate survival mechanisms. However, inflammation can also contribute to several pathologies, particularly under chronic hypoxia [5]. As altitude increases, the decreased barometric pressure leads to a decreased oxygen partial pressure (PO_2) and triggers hypobaric hypoxic challenge. As compared to other hypoxic conditions, such as hypoxic-ischemic tissue damage, intermittent hypoxia and obstructive sleep apnea, and hypoxic tumor microenvironment, high-altitude hypoxia is a systemic hypoxemia distinguished by its combination of low PO_2 and hypobaric environment, which has been widely used for studying adaptation/maladaptation to acute, subacute, or chronic hypoxia [5]. Clinically, the first three days following arrival at a high altitude are termed the acute exposure phase, days 3–14 represent the subacute exposure period, and exposure lasting several months to years constitutes the chronic phase [2]. In the present study, we observed a dynamic inflammatory response in both plasma and monocytes from Human participants exposed to a high altitude of 5500m, but did not exhibit any symptoms related to AMS. Cytokine levels significantly increased after acute exposure but returned to baseline after prolonged (30-day) exposure. This result suggested that the inflammation induced by acute hypoxia is transient and self-resolving with prolonged exposure duration in healthy climbers. There is a general consensus that pro-inflammatory cytokines and other inflammatory markers are increased in individuals acutely exposed to high altitude. However, in some cases, inflammatory mediator expression appears to differ between individuals who develop AMS and those who do not. For example, patients with AMS show increased plasma levels of IL-1β, IL-6, and TNF-α but decreased IL-10 compared to non-AMS controls. In addition, the correlation between plasma IL-6 and AMS score has been established by multiple independent studies [5, 30]. Furthermore, in those high-altitude human populations, several inflammation-related genes, such as *IL6*, *IL1A*, *IL1B*, *NOS1*, *NOS2*, and *TNF*, have been identified as top candidates showing signals of evolutionary selection [5]. Therefore, the spontaneous and timely alleviation of inflammation could prevent the pathogenesis of AMS. Consistently, other hypoxia-induced physiological responses, including enhanced sympathetic activity and pulmonary vasoconstriction, are also gradually normalized with prolonged exposure to high altitude in non-AMS climbers [31].

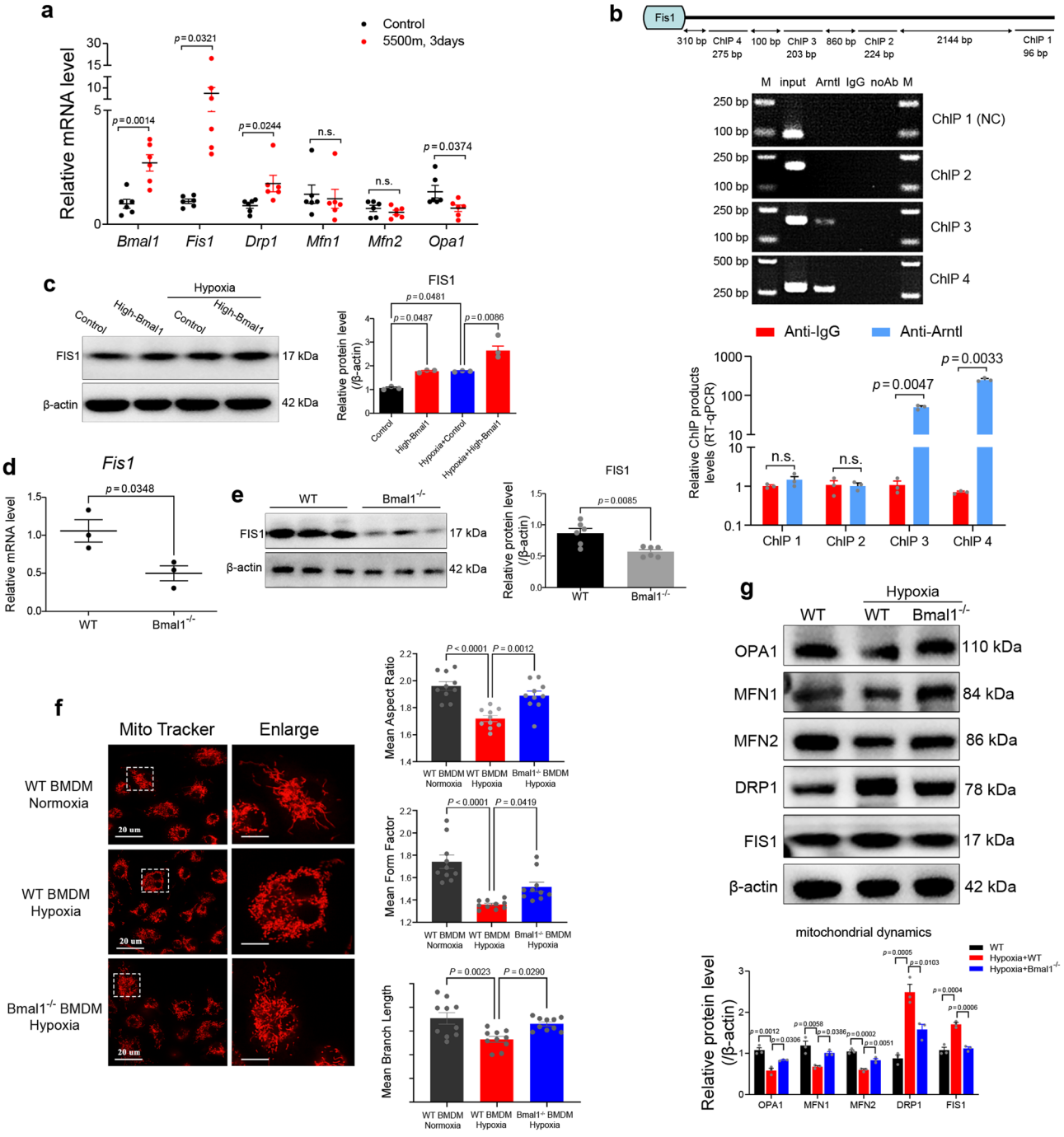

Fig. 5 BMAL1 stabilized mitochondrial protein homeostasis by targeting *Fis1* transcription in monocytes. **A** RT-qPCR analysis showed the mRNA-expression levels of *Bmal1*, mitochondrial fission genes (*Fis1* and *Drp1*), and mitochondrial fusion genes (*Mfn1*, *Mfn2*, and *Opa1*) in PBMCs from mice exposed to a simulated altitude of 5500 m for 0 or 3 days (n = 6). **B** ChIP assays for BMAL1 enrichment at the *Fis1* promoter region in RAW264.7 cells. RT-PCR (upper) and RT-qPCR (lower) analyses of ChIP products using four pairs of amplification primers (including a pair of control primers) (n = 3). **C** Western blot analysis of FIS1-protein levels in *Bmal1*-overexpressing RAW264.7, cultured under normal (21% oxygen) or hypoxic (1% oxygen) conditions for 24 h (n = 3). **D, E,** Fis1 mRNA expression (**D**) and protein levels (**E**) in Bmal1$^{-/-}$ and WT BMDMs cultured under 1% oxygen for 24 h (n = 3). **F, G,** Mean aspect ratio, form factor, and branch length of the mitochondria labeled with Mito-Tracker Red (scale bars = 20 μm, **F**); western blot analysis showed the levels of mitochondrial fission proteins (FIS1 and DRP1) and mitochondrial fusion proteins (MFN1, MFN2, and OPA1, **G**) in Bmal1$^{-/-}$ and WT BMDMs cultured under 1% oxygen for 0 or 24 h (n = 3). Smaller aspect ratio, form factor, and branch length values represent increased mitochondrial fragmentation (n = 10). The data shown represent the mean ± SEM. Statistical significance was determined by performing unpaired Student's two-tailed t test with Welch's correction (**A, B, D, E**) or 1-way ANOVA followed by Tukey's multiple-comparisons test (**C, F, G**). Abbreviation: bp, base pairs

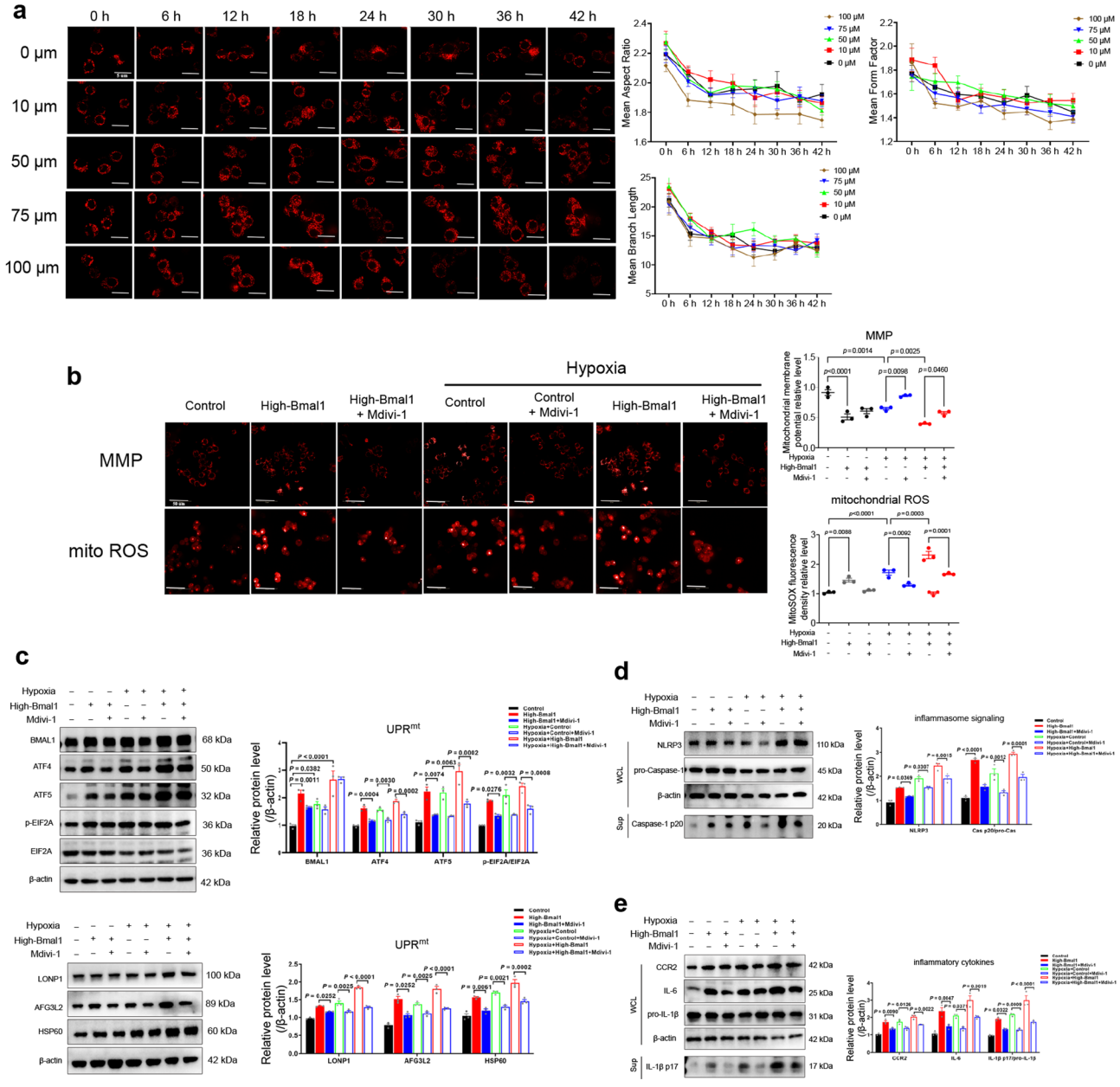

Fig. 6 Inhibition of mitochondrial fission alleviated *Bmal1* overexpression-induced UPR^{mt} and inflammation in monocytes under hypoxia. **A** RAW264.7 cells were treated with a mitochondrial fission inhibitor (Mdivi-1) at the different concentrations (0, 10, 50, 75, or 100 μM). MitoTracker^{TM} staining was used to detect and quantify dynamic changes in mitochondrial fragmentation in RAW264.7 cells after 0–42 h of Mdivi-1 treatment (n = 3, scale bars = 5 μm). **B–E***Bmal1*-overexpressing RAW264.7 cells were treated with 50 μM Mdivi-1 and cultured under 21% oxygen (normal condition) or 1% oxygen (hypoxic condition) for 24 h. Fluorescent probe staining was performed to quantify MMP (upper) and mitochondrial ROS (lower) levels (scale bar = 50 μm, **B**). Western blot analysis revealed the protein-expression levels of UPR^{mt} markers (ATF4, ATF5, p-EIF2A/EIF2A, LONP1, HSP60, and AFG3L2, **C**), NLRP3 inflammasome-signaling proteins (NLRP3, Caspase-1 p20/pro-Caspase-1, **D**) and inflammatory cytokines (CCR2, IL-6 and IL-1β p17/pro-IL-1β, **E**) in RAW264.7 cells (n = 3). The data shown represent the mean ± SEM. Statistical significance was determined by performing 1-way ANOVA with Tukey's multiple-comparisons test (**B–E**). Abbreviation: WCL, whole cell lysate; Sup, supernatant

Monocytes are central players in the innate immune system that exhibit highly diverse responses to environmental cues [32, 33]. The bioinformatics and confirmatory analyses conducted in this study indicated that *Bmal1* correlated significantly and positively with inflammation in human PBMCs after exposure to high-altitude hypoxia. The mammalian circadian clock mechanism is cell-autonomous and regulates tissue-specific rhythmic functions through transcription-translation negative-feedback loops [13]. In addition, the circadian clock participates in the development of various diseases through key TFs [13, 34]. In myeloid cells, BMAL1 has been found

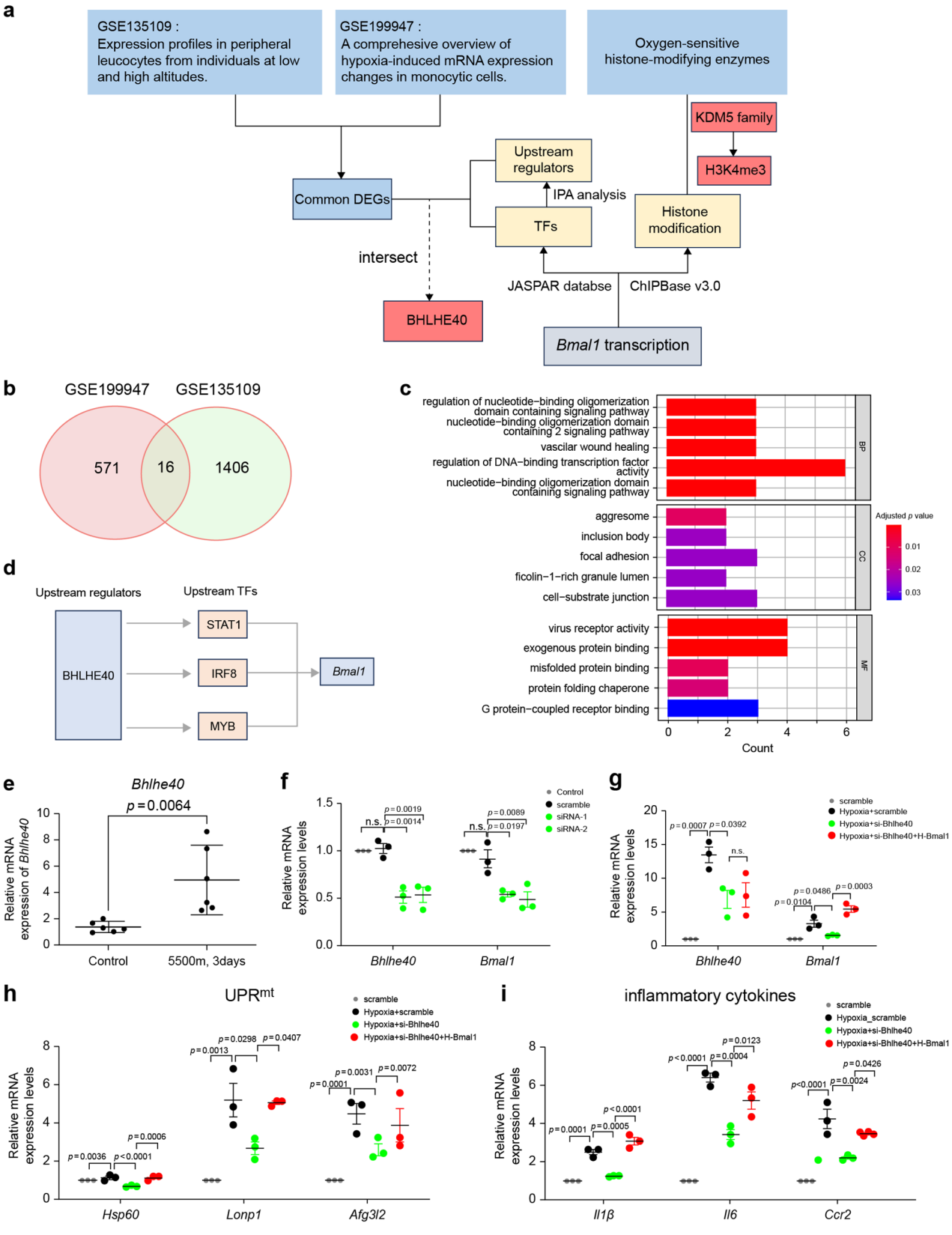

Fig. 7 (See legend on next page.)

(See figure on previous page.)

Fig. 7 TF, BHLHE40, stimulated Bmal1 transcription in monocytes under hypoxia. A Flowchart of bioinformatics analysis used to identify potential regulators of Bmal1 transcriptional activation under hypoxia. B Venn diagram of common DEGs between the GSE135109 and GSE199947 datasets. C GO pathway-enrichment analysis of 16 common genes. D Diagram of the predicted regulatory pathways associated with BHLHE40 and Bmal1 transcription. E Bmal1 mRNA expression was investigated via RT-qPCR analysis in RAW264.7 cells transfected with Bhlhe40 siRNAs and untransfected RAW264.7 cells (n = 3). F Bhlhe40mRNA expression was investigated by RT-qPCR analysis in PBMCs from mice subjected to a simulated altitude of 5500 m for 0 or 3 days (n = 6). G–I Bmal1-overexpressing RAW264.7 cells were transfected with siRNAs to inhibit Bhlhe40 expression and then cultured under 1% oxygen (hypoxic condition) for 24 h. RT-qPCR analysis showed the mRNA-expression levels of Bmal1(G), UPRmt markers (Lonp1,Hsp60, and Afg3l2, H),and inflammatory cytokines(Il6,Mcp1, and Il1β, I) in RAW264.7 cells (n = 3).Statistical significance was determined by performing an unpaired Student's two-tailed t test with Welch's correction (E) or 1-way ANOVA followed by Tukey-s multiple-comparisons tests

to control monocyte diurnal oscillations [26], macrophage functions [35], and inflammatory cytokine production [26, 36, 37]. In this study, M-BKO mice showed significantly lower inflammatory activity related to monocytes and circulating inflammation.

Accumulating evidence indicates that organisms lacking an intrinsic clock may be less vulnerable to environmental disturbances, which may have beneficial effects under certain stressed conditions [38, 39]. For example, global *Bmal1* knockout in adulthood can facilitate adaptation to light/dark disruption and protect mice from atherosclerosis and insulin resistance [40, 41]. In addition, smooth muscle-specific *Bmal1* knockout protected mice from abdominal aortic aneurysm [42], and myeloid-specific *Bmal1* knockout reduced the aortic inflammatory response and retarded atherogenesis [38]. Our current findings suggest that knocking out *Bmal1* in monocytes can potentially serve as a novel therapeutic approach for alleviating inflammation induced by high-altitude hypoxia.

UPR^{mt} and NLRP3 inflammasome signaling in monocytes were responsible for inflammatory responses during high-altitude hypoxia

Mitochondria orchestrate myriad biological functions including oxygen homeostasis, energy production, metabolism, and inflammation. To maintain mitochondrial protein homeostasis, molecular chaperones and proteases cooperate to ensure appropriate folding of newly imported proteins and degradation of misfolded or nonfunctional proteins in the mitochondrial matrix [43]. Upon proteotoxic stress, a nuclear transcriptional response (the UPR^{mt}), which promotes expression of the mitochondrial chaperone HSP60 and the proteases LONP1 and AFG3L2, is activated to repair and recover protein homoeostasis in mitochondria [43]. Long-term and constitutive UPR^{mt} activation promotes the release of mitochondrial damage-associated molecular patterns and activates pattern-recognition receptors, which trigger inflammatory reactions by stimulating cyclic GMP–AMP synthase and inflammasome signaling [6]. Inflammasomes are complex inflammatory signaling platforms responsible for IL-1β and IL-18 release through caspase-1 activation [44]. Mitochondria are sensitive to decreased oxygen availability, and the present findings demonstrated that mitochondrial protein homeostasis was severely impaired in human PBMCs exposed to high-altitude hypoxia. In human participants and mouse models, the expression of UPR^{mt}-related genes in monocyte-enriched PBMCs was significantly enhanced, accompanied by mitochondrial dysfunction (mitochondrial ROS production and MMP depolarization) during acute high-altitude hypoxia, whereas it gradually decreased to baseline levels during prolonged high-altitude hypoxia. Furthermore, UPR^{mt} activation stimulated NLRP3 inflammasomes and IL1β inflammatory signaling in monocytes.

TF, BMAL1, promoted the UPR^{mt} by targeting Fis1 in monocytes during high-altitude hypoxia

Mitochondria continuously fuse and divide to control their size, number, and morphology [24]. The dynamic equilibrium of the mitochondrial fission–fusion cycle is controlled by the circadian clock [23–25], which is highly sensitive to hypoxic stress [45, 46]. BMAL1 binds to the promoter E-box elements *Fis1*, *Bnip3*, *Pink1*, and *Mtfr1* in cardiomyocytes and hepatocytes [47, 48]. In this study, ChIP assay and gain/loss-of-function experiments confirmed that BMAL1 bound the promoter region of *Fis1* and favored mitochondrial fission in monocytes. In addition, *Bmal1* overexpression induced UPR^{mt} and NLRP3 inflammasome activation, whereas inhibiting mitochondrial fission with Mdivi-1 significantly alleviated BMAL1-induced mitoinflammation in monocytes under hypoxic conditions.

BHLHE40, a stress-responsive TF, stimulated Bmal1 transcription in monocytes during high-altitude hypoxia

Epigenetic chromatin modifications and TF binding to promoters represent two crucial mechanisms for the transcriptional activation of circadian clock genes [13]. KDM5 histone demethylases belong to a family of oxygen-dependent dioxygenases that epigenetically regulate gene transcription in response to hypoxic stress by targeting H3K4me1/2/3 [49]. In this study, we found that H3K4me1/2/3 were activated in monocytes during high-altitude hypoxia. However, inhibiting KDM5 demethylase activity or KDM5A/5C gene expression did not promote *Bmal1* transcription, suggesting that the KDM5 histone demethylase family does not promote *Bmal1*

Table 1 Predicted upstream TFs of *Bmal1*

Symbol	Symbol	Symbol	Symbol
GATA3	FOXD2	IRF3	KLF16
TRPS1	BCL11B	IRF8	KLF11
NR2F2	HSF1	IRF9	KLF15
MYOD1	HSF2	CDX1	SP8
SNAI2	HSF4	CDX2	SP9
SNAI3	REST	HOXA10	PATZ1
MYB	ZIC1	CDX4	SP1
RFX4	NR2F2	HOXD9	KLF1
ONECUT1	NR2F6	ZNF701	SP2
ZNF24	IRF2	TEAD1	SP4
NFIC	IRF4	MEIS1	KLF14
ZNF549	IRF1	LHX2	KLF12
MGX	ZKSCAN1	KLF9	KLF10
EVX1	NR1H2	ZNF281	KLF7
FOXD3	NR4A1	SP3	WT1
FOXJ3	STAT2	KLF5	ZNF740
FOXC2	STAT1	KLF16	RREB1

[a]Based on the JASPAR database, 68 upstream TFs were predicted to act on the upstream 2000-base pair promoter region of *Bmal1*

Table 2 Prediction of histone modifications in regulatory regions of *Bmal1*

Histone modification	Number of samples found		Number of binding sites	
	upstream	downstream	Upstream	downstream
H1.0	0	1	0	1
H1.4	1	2	1	2
H2A	5	3	5	3
H2AFZ	14	13	14	14
H2AK9ac	1	1	1	2
H2AZ	5	1	6	1
H2BK120ac	1	1	1	1
H2BK5ac	2	2	2	2
H3F3A	4	1	4	2
H3K14ac	0	3	0	4
H3K18ac	3	10	3	13
H3K23ac	2	2	2	4
H3K23me2	1	2	1	3
H3K27ac	10	11	10	11
H3K27me1	0	1	0	1
H3K4me1	3	1	3	1
H3K4me2	20	22	20	22
H3K4me3	9	37	9	38
H3K4me3B	1	1	1	1
H3K9ac	11	12	11	13
H3K9me3	1	0	1	0
H3ac	2	2	2	4
H4	0	1	0	1
H4K20me1	0	3	0	3
H4K20me3	0	1	0	1
H4K5ac	1	2	1	2
H4K8ac	2	3	3	5
H4K91ac	1	3	1	3
H4ac	1	3	1	3

[a]Based on ChIPBase v3.0 (https://rnasysu.com/chipbase3/index.php), 29 types of histone modifications were predicted to occur in the regulatory regions of *Bmal1*

transcription during hypoxia. In contrast, we found that BHLHE40, a critical TF, stimulated *Bmal1* transcription during hypoxia, based on a series of bioinformatic analyses and confirmation experiments. BHLHE40 can recognize DNA motifs known as E-boxes (CANNTG), served as an important hypoxia biomarker, and is directly regulated by HIF-1α [50, 51]. In this study, BHLHE40 acted as an upstream regulator of *Bmal1* transcription under high-altitude hypoxia, thereby driving the UPR^{mt} and inflammatory responses in monocytes.

Practical implications and limitations of this study

Circadian clocks sense environmental signals, including light, temperature, and nutrients [52]. Hypoxic signaling can engage in crosstalk with circadian clocks, suggesting that oxygen may to serve as a resetting cue (a zeitgeber) [11, 53]. For example, HIF-1α and BMAL1 (core regulators of hypoxia and circadian clock signaling) have been demonstrated to share structural similarity and interact directly to cross-regulate each other. However, the underlying molecular mechanisms remain unclear. The present findings clearly indicate that BHLHE40, an HIF-1α-related TF, directly targeted the *Bmal1* promoter to promote its transcription, providing direct evidence that hypoxic signaling could be a novel resetting zeitgeber. In addition, we found that *Bmal1* deletion significantly alleviated inflammatory responses, suggesting a novel approach for modulating the intrinsic clock to render organisms less vulnerable to environmental stress.

The present study has some limitations. First, although we primarily focused on monocytes/macrophages, the abundance of other immune cell types within human whole blood, such as $CD4^+$ and $CD8^+$ T cells, was also significantly altered in the high-altitude group compared with the sea-level group (Additional File 1: Figure S1). $CD4^+$ T-cells are usually referred to as helper T-cells, which secrete various cytokines to assist other immune cells and coordinate the overall immune response. $CD8^+$ T-cells, also known as cytotoxic T lymphocytes, directly recognize antigens and kill abnormal cells. $CD4^+$ and $CD8^+$ T-cells generally function synergistically to maintain the body's immune defense functions, but further research is required to explore the specific roles of $CD4^+$ and $CD8^+$ T-cells in the inflammation induced by high-altitude hypoxia. Second, the expression levels of clock genes, including *Bmal1*, *Per2*, *Nr1d1*, *Clock*, and *Cry1*, normally follows circadian oscillation, and exhibit diurnal variations in amplitude among individuals. Although we analyzed the mRNA expression of these clock genes in PBMCs at 5500 m for 3 or 30 days, we did not quantify

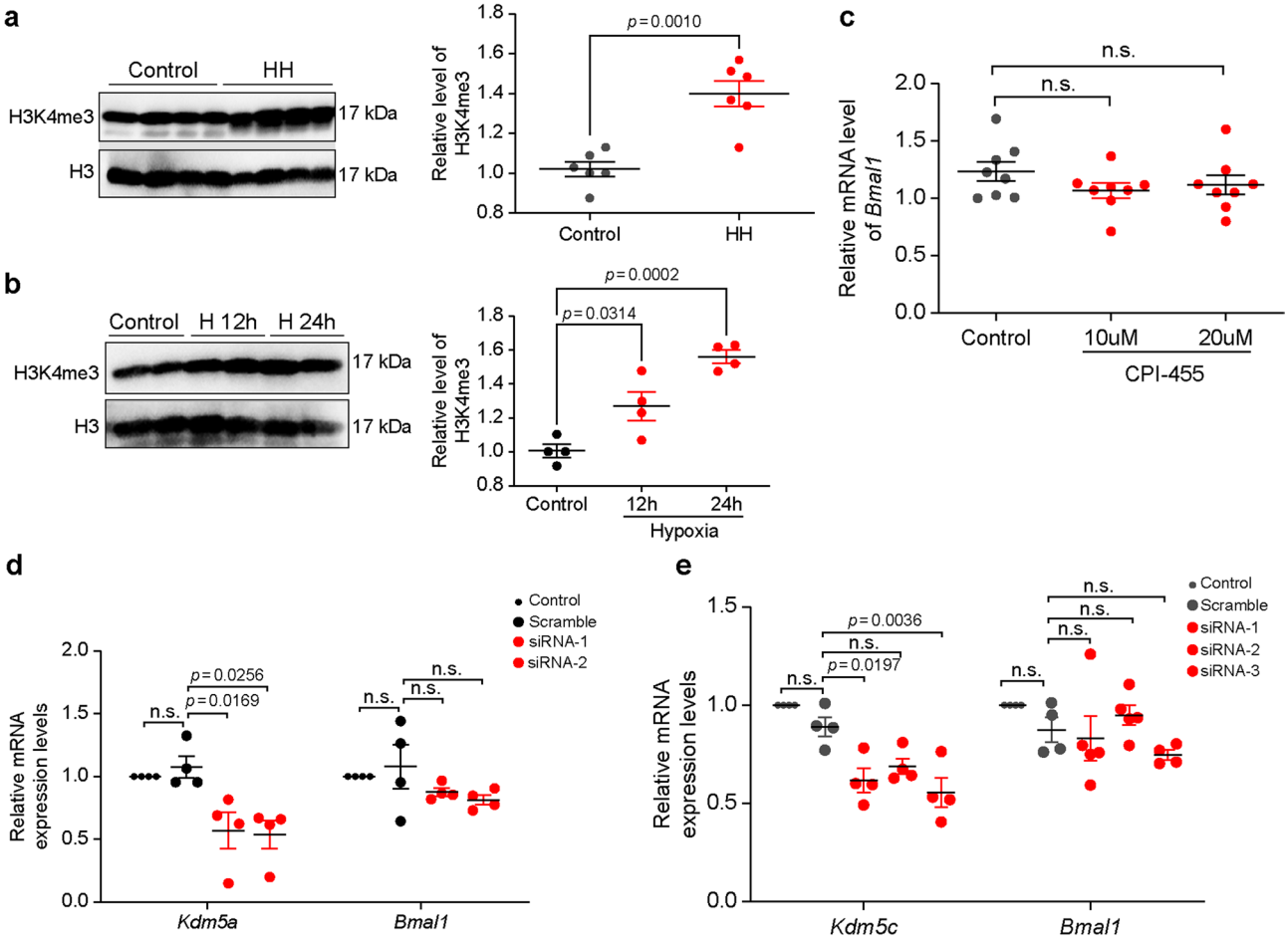

Fig. 8 KDM5 histone demethylases did not drive the transcriptional activation of *Bmal1* in monocytes under hypoxia. **A, B** Western blot analysis showed H34Kme3 protein levels in PBMCs from mice exposed to a simulated altitude of 5500 m for 0 or 3 days (n = 6, **A**) and in the RAW264.7 cells cultured under 1% oxygen (hypoxic condition) for 12 h or 24 h (n = 3, **B**).**C** RT-qPCR analysis showed *Bmal1* mRNA-expression levels in RAW264.7 cells treated with CPI-455 (a KDM5-demethylase family inhibitor) at concentrations of 10 or 20 μM for 24 h (n = 3). **D, E**, RT-qPCR analysis of *Bmal1* mRNA-expression levels in RAW264.7 cells transfected with *Kdm5a* (**D**) or *Kdm5c* (**E**) siRNAs (n = 3). Statistical significance was determined by performing anunpaired Student's two-tailed t test with Welch's correction (**A**) or 1-way ANOVA followed by Tukey's multiple-comparisons test (**B–E**)

key rhythmic parameters, such as oscillation period, amplitude, or phase. Additionally, all the human and murine subjects in this study were male; hence, the loss of sex-based effects has not been avoided, and more evidence from female samples is needed from future studies.

Conclusions

In conclusion, BHLHE40, a hypoxic stress-responsive TF, directly promoted *Bmal1* transcription and induced NLRP3 inflammasome activation in monocytes by targeting *Fis1*-mediated UPR^{mt}. In contrast, the inhibiting or deleting *Bmal1* alleviated the inflammatory response in circulating plasma and monocytes under high-altitude hypoxia. Our results provide novel insight, suggesting that modulating the intrinsic clock could render organisms less vulnerable to environmental stress and protect them from hypoxia.

Abbreviations

$\|log_2FC\|$	absolute log_2 fold-change
AFG3L2	AFG3-like AAA ATPase 2
AFMU	Air Force Medical University
AMS	acute mountain sickness
ANOVA	analysis of variance
BHLHE40	basic helix-loop-helix family member E40
BMDM	Bone marrow-derived macrophage
BMLA1	brain and muscle Arnt-like protein 1
bp	base pairs
CCR2	C-C motif chemokine receptor 2
ChIP	chromatin immunoprecipitation
DEG	differentially expressed gene
DRP1	dynamin-related protein 1
ELISA	enzyme-linked immunosorbent assay
Fis1	fission 1
GO	Gene Ontology
HIF	hypoxia-inducible factor
High-BMAL1 cells	cells overexpressing BMAL1
HSP60	heat shock protein 60
IL	interleukin
KEGG	Kyoto Encyclopedia of Genes and Genomes
LONP1	lon peptidase 1
LyC6	lymphocyte antigen 6 C

M-BKO	myeloid-specific Bmal1 knockout
Mdivi-1	mitochondrial division inhibitor-1
MFIM	multichannel fluorescence intravital microscopy
MFN	mitofusin
MMP	mitochondrial membrane potential
mtROS	mitochondrial reactive oxygen species
NLRP3	NOD-like receptor protein 3
OPA	optic atrophy
ROS	reactive oxygen species
RT-PCR	reverse transcriptase-polymerase chain reaction
RT-qPCR	reverse transcriptase-quantitative polymerase chain reaction
SEM	standard error of the mean
siRNA	small-interfering RNA
TF	transcription factor
UPR^{mt}	mitochondrial unfolded protein response
WT	wild-type

Supplementary Information

The online version contains supplementary material available at https://doi.org/10.1186/s12964-025-02420-8.

Additional File 1. docx Figure S1.Immune cell landscape of human whole blood at a high altitude. Figure S2**.** Expression of clock genes in monocytes during 3- and 30-day exposure to high-altitude hypoxia. Figure S3**.**Flow-plots demonstrating the flow-cytometry sorting strategy for monocytes. Figure S4**.**Analysis of mitochondria-related DEGs in mouse PBMCs under acute high-altitude hypoxia. Figure S5**.**Significant NLRP3 and IL-1β mRNA expression upregulation under high-altitude hypoxia. Figure S6. Knockdown or overexpression of ***Bmal1*** modulated the UPR^{mt} and NLRP3 inflammasome activation in monocytes under hypoxia. Figure S7**.** DEG analyses using the GSE135109 and GSE199947 datasets. Figure S8**.**Effects of modulating HIF signaling pathways on ***Bhlhe40*** transcription in various cell types. Table S1. Antibodies used for immunoblotting or immunofluorescence. Table S2**.** Sequences of primers used for RT-qPCR. Table S3. Sequences of primers used for ChIP assays. Table S4**.** Dynamic changes of inflammatory cytokine levels in human plasma at 5500 m. Table S5. Common genes between identified DEGs and mouse mitochondrial gene set of Mouse MitoCarta3.0. Table S6. Intersecting DEGs under hypoxia (GSE135109 and GSE199947). Table S7. Predicted upstream regulators of TFs targeting ***Bmal1*****.**

Additional File 2. mp4 Video S1. Monocytic cell adhesion and infiltration into the pulmonary vasculature in mice under acute high-altitude hypoxia.

Additional File 3.Original videos of each N number in Fig.2F and Video S1.

Additional File 4.Original western blot images.

Acknowledgements
Not applicable.

Authors' contributions
MJX, XWC, and YL designed and conceptualized the study. YLG, JX, and YC performed the experiments, prepared figures, and wrote the manuscript. BZ, JX, SYH., and PJL contributed to the experiments. YRB, LZ, ZBY and HM supervised the study and prepared the manuscript. All authors read and approved the final manuscript.

Funding
This study was supported by funding from the National Natural Science Foundation of China (grant number 82072101, Man-Jiang Xie) and National Key Research and Development Program of China (grant numbers 2020YFA0803603 and 2021YFA1301402, Yong Liu). The sponsors had no role in the conceptualization, design, data collection, analysis, decision to publish, or preparation of the manuscript.

Data availability
All data generated or analyzed during this study are included in this published article and its supplementary information files.

Declarations

Ethics approval and consent to participate
The study protocol was approved by the Human Research Ethics Committee of the Air Force Medical University (AFMU) (approval number ChiCLR2000037401) and was conducted in accordance with the principles of the Declaration of Helsinki. All participants provided written informed consent to participate in the study after reading information about the study and explaining the procedures to them. The animal study protocol was approved by the Animal Care and Use Committee of AFMU, protocol number 250625. The study adhered to the guidelines set by the committee.

Consent for publication
Not applicable.

Competing interests
The authors declare that they have no competing interests.

Author details
[1]Department of Aerospace Physiology, Key Laboratory of Aerospace Medicine of Ministry of Education, Air Force Medical University, 169 Changle West Road, Xi'an, Shaanxi Province 710032, China
[2]China Astronaut Research and Training Center, Beijing 100094, China
[3]Department of Cardiology, Xijing Hospital, Air Force Medical University, Xi'an, Shaanxi Province 710032, China
[4]Department of Physiology, Department of Pathophysiology, School of Basic Medical Sciences, Air Force Medical University, Xi'an, Shaanxi Province 710032, China
[5]School of Pharmacy, Tianjin Medical University, Tianjin 300070, China

Received: 23 April 2025 / Accepted: 27 August 2025
Published online: 08 October 2025

References

1. Netzer N, Strohl K, Faulhaber M, Gatterer H, Burtscher M. Hypoxia-related altitude illnesses. J Travel Med. 2013;20:247–55. https://doi.org/10.1111/jtm.12017.
2. Richalet JP, Hermand E, Lhuissier FJ. Cardiovascular physiology and pathophysiology at high altitude. Nat Rev Cardiol. 2024;21:75–88. https://doi.org/10.1038/s41569-023-00924-9.
3. Gatterer H, Villafuerte FC, Ulrich S, Bhandari SS, Keyes LE, Burtscher M. Altitude illnesses. Nat Rev Dis Primers. 2024;10:43. https://doi.org/10.1038/s41572-024-00526-w.
4. El Alam S, Pena E, Aguilera D, Siques P, Brito J. Inflammation in pulmonary hypertension and edema induced by hypobaric hypoxia exposure. Int J Mol Sci. 2022;23:12656. https://doi.org/10.3390/ijms232012656.
5. Pham K, Parikh K, Heinrich EC. Hypoxia and inflammation: insights from high-altitude physiology. Front Physiol. 2021;12:676782. https://doi.org/10.3389/fphys.2021.676782.
6. Marchi S, Guilbaud E, Tait SWG, Yamazaki T, Galluzzi L. Mitochondrial control of inflammation. Nat Rev Immunol. 2023;23:159–73. https://doi.org/10.1038/s41577-022-00760-x.
7. Schmitt K, Grimm A, Dallmann R, Oettinghaus B, Restelli LM, Witzig M, et al. Circadian control of DRP1 activity regulates mitochondrial dynamics and bioenergetics. Cell Metab. 2018;27:657–e6665. https://doi.org/10.1016/j.cmet.2018.01.011.
8. Rabinovich-Nikitin I, Rasouli M, Reitz CJ, Posen I, Margulets V, Dhingra R, et al. Mitochondrial autophagy and cell survival is regulated by the circadian clock gene in cardiac myocytes during ischemic stress. Autophagy. 2021;17:3794–812. https://doi.org/10.1080/15548627.2021.1938913.
9. Jin Z, Ji Y, Su W, Zhou L, Wu X, Gao L, et al. The role of circadian clock-controlled mitochondrial dynamics in diabetic cardiomyopathy. Front Immunol. 2023;14:1142512. https://doi.org/10.3389/fimmu.2023.1142512.
10. Partch CL, Green CB, Takahashi JS. Molecular architecture of the mammalian circadian clock. Trends Cell Biol. 2014;24:90–9. https://doi.org/10.1016/j.tcb.2013.07.002.
11. Scheiermann C, Kunisaki Y, Frenette PS. Circadian control of the immune system. Nat Rev Immunol. 2013;13:190–8. https://doi.org/10.1038/nri3386.
12. Sartor F, Ferrero-Bordera B, Haspel J, Sperandio M, Holloway PM, Merrow M. Circadian clock and hypoxia. Circ Res. 2024;134:618–34. https://doi.org/10.1161/CIRCRESAHA.124.323518.

13. Liu XL, Duan Z, Yu M, Liu X. Epigenetic control of circadian clocks by environmental signals. Trends Cell Biol. 2024;34:992–1006. https://doi.org/10.1016/j.tcb.2024.02.005.
14. Manella G, Ezagouri S, Champigneulle B, Gaucher J, Mendelson M, Lemarie E, et al. The human blood transcriptome exhibits time-of-day-dependent response to hypoxia: lessons from the highest city in the world. Cell Rep. 2022;40:111213. https://doi.org/10.1016/j.celrep.2022.111213.
15. Ying W, Cheruku PS, Bazer FW, Safe SH, Zhou B. Investigation of macrophage polarization using bone marrow derived macrophages. J Vis Exp. 2013;7650323. https://doi.org/10.3791/50323.
16. Lu B, Wang S, Feng H, Wang J, Zhang K, Li Y, et al. FERONIA-mediated TIR1/AFB2 oxidation stimulates auxin signaling in *Arabidopsis*. Mol Plant. 2024;17:772–87. https://doi.org/10.1016/j.molp.2024.04.002.
17. Cretin E, Lopes P, Vimont E, Tatsuta T, Langer T, Gazi A, et al. High-throughput screening identifies suppressors of mitochondrial fragmentation in *OPA1* fibroblasts. EMBO Mol Med. 2021;13:e13579. https://doi.org/10.15252/emmm.202013579.
18. Chen L, Zhang B, Yang L, Bai YG, Song JB, Ge YL, et al. BMAL1 disrupted intrinsic diurnal oscillation in rat cerebrovascular contractility of simulated microgravity rats by altering circadian regulation of miR-103/Ca_v1.2 signal pathway. Int J Mol Sci. 2019;20:3947. https://doi.org/10.3390/ijms20163947.
19. Zhao D, Zhong G, Li J, Pan J, Zhao Y, Song H, et al. Targeting E3 ubiquitin ligase WWP1 prevents cardiac hypertrophy through destabilizing DVL2 via inhibition of K27-linked ubiquitination. Circulation. 2021;144:694–711. https://doi.org/10.1161/CIRCULATIONAHA.121.054827.
20. Yi H, Yu Q, Zeng D, Shen Z, Li J, Zhu L, et al. Serum inflammatory factor profiles in the pathogenesis of high-altitude polycythemia and mechanisms of acclimation to high altitudes. Mediators Inflamm. 2021;2021:8844438. https://doi.org/10.1155/2021/8844438.
21. Kammerer T, Faihs V, Hulde N, Stangl M, Brettner F, Rehm M, et al. Hypoxic-inflammatory responses under acute hypoxia: in vitro experiments and prospective observational expedition trial. Int J Mol Sci. 2020;21:1034. https://doi.org/10.3390/ijms21031034.
22. O'Malley J, Kumar R, Inigo J, Yadava N, Chandra D. Mitochondrial stress response and cancer. Trends Cancer. 2020;6:688–701. https://doi.org/10.1016/j.trecan.2020.04.009.
23. Murphy MP, O'Neill LAJ. A break in mitochondrial endosymbiosis as a basis for inflammatory diseases. Nature. 2024;626:271–9. https://doi.org/10.1038/s41586-023-06866-z.
24. Harrington JS, Ryter SW, Plataki M, Price DR, Choi AMK. Mitochondria in health, disease, and aging. Physiol Rev. 2023;103:2349–422. https://doi.org/10.1152/physrev.00058.2021.
25. Kim SH, Shin HJ, Yoon CM, Lee SW, Sharma L, Dela Cruz CS, et al. PINK1 inhibits multimeric aggregation and signaling of MAVS and MAVS-dependent lung pathology. Am J Respir Cell Mol Biol. 2021;64:592–603. https://doi.org/10.1165/rcmb.2020-0490OC.
26. Nguyen KD, Fentress SJ, Qiu Y, Yun K, Cox JS, Chawla A. Circadian gene Bmal1 regulates diurnal oscillations of Ly6C^{hi} inflammatory monocytes. Science. 2013;341:1483–8. https://doi.org/10.1126/science.1240636.
27. Shimada K, Crother TR, Karlin J, Dagvadorj J, Chiba N, Chen S, et al. Oxidized mitochondrial DNA activates the NLRP3 inflammasome during apoptosis. Immunity. 2012;36:401–14. https://doi.org/10.1016/j.immuni.2012.01.009.
28. Park S, Juliana C, Hong S, Datta P, Hwang I, Fernandes-Alnemri T, et al. The mitochondrial antiviral protein MAVS associates with NLRP3 and regulates its inflammasome activity. J Immunol. 2013;191:4358–66. https://doi.org/10.4049/jimmunol.1301170.
29. Sinha KK, Bilokapic S, Du Y, Malik D, Halic M. Histone modifications regulate pioneer transcription factor cooperativity. Nature. 2023;619:378–84. https://doi.org/10.1038/s41586-023-06112-6.
30. Schoene RB, Hackett PH, Henderson WR, Sage EH, Chow M, Roach RC, et al. High-altitude pulmonary edema. Characteristics of lung lavage fluid. JAMA. 1986;256:63–9. https://doi.org/10.1001/jama.1986.03380010067027.
31. Luks AM, Swenson ER, Bärtsch P. Acute high-altitude sickness. Eur Respir Rev. 2017;26:160096. https://doi.org/10.1183/16000617.0096-2016.
32. Gordon S, Taylor PR. Monocyte and macrophage heterogeneity. Nat Rev Immunol. 2005;5:953–64. https://doi.org/10.1038/nri1733.
33. Jakubzick CV, Randolph GJ, Henson PM. Monocyte differentiation and antigen-presenting functions. Nat Rev Immunol. 2017;17:349–62. https://doi.org/10.1038/nri.2017.28.
34. Zheng Y, Pan L, Wang F, Yan J, Wang T, Xia Y, et al. Neural function of Bmal1: an overview. Cell Biosci. 2023;13:1. https://doi.org/10.1186/s13578-022-00947-8.
35. Oishi Y, Hayashi S, Isagawa T, Oshima M, Iwama A, Shimba S, et al. Bmal1 regulates inflammatory responses in macrophages by modulating enhancer RNA transcription. Sci Rep. 2017;7:7086. https://doi.org/10.1038/s41598-017-07100-3.
36. Early JO, Menon D, Wyse CA, Cervantes-Silva MP, Zaslona Z, Carroll RG, et al. Circadian clock protein BMAL1 regulates IL-1β in macrophages via NRF2. Proc Natl Acad Sci U S A. 2018;115:E8460-8. https://doi.org/10.1073/pnas.1800431115.
37. Huo M, Cao X, Zhang H, Lau CW, Hong H, Chen FM, et al. Loss of myeloid Bmal1 exacerbates hypertensive vascular remodelling through interaction with STAT6 in mice. Cardiovasc Res. 2022;118:2859–74. https://doi.org/10.1093/cvr/cvab336.
38. Yang G, Zhang J, Jiang T, Monslow J, Tang SY, Todd L, et al. Bmal1 deletion in myeloid cells attenuates atherosclerotic lesion development and restrains abdominal aortic aneurysm formation in hyperlipidemic mice. Arterioscler Thromb Vasc Biol. 2020;40:1523–32. https://doi.org/10.1161/ATVBAHA.120.314318.
39. Bunger MK, Wilsbacher LD, Moran SM, Clendenin C, Radcliffe LA, Hogenesch JB, et al. Mop3 is an essential component of the master circadian pacemaker in mammals. Cell. 2000;103:1009–17. https://doi.org/10.1016/s0092-8674(00)00205-1.
40. Yang G, Chen L, Grant GR, Paschos G, Song WL, Musiek ES, et al. Timing of expression of the core clock gene Bmal1 influences its effects on aging and survival. Sci Transl Med. 2016;8:324ra16. https://doi.org/10.1126/scitranslmed.aad3305.
41. Yang G, Chen L, Zhang J, Ren B, FitzGerald GA. Bmal1 deletion in mice facilitates adaptation to disrupted light/dark conditions. JCI Insight. 2019;5:e125133. https://doi.org/10.1172/jci.insight.125133.
42. Lutshumba J, Liu S, Zhong Y, Hou T, Daugherty A, Lu H, et al. Deletion of *BMAL1* in smooth muscle cells protects mice from abdominal aortic aneurysms. Arterioscler Thromb Vasc Biol. 2018;38:1063–75. https://doi.org/10.1161/ATVBAHA.117.310153.
43. Sutandy FXR, Gößner I, Tascher G, Münch C. A cytosolic surveillance mechanism activates the mitochondrial UPR. Nature. 2023;618:849–54. https://doi.org/10.1038/s41586-023-06142-0.
44. Wang Y, Liu X, Shi H, Yu Y, Yu Y, Li M, et al. NLRP3 inflammasome, an immune-inflammatory target in pathogenesis and treatment of cardiovascular diseases. Clin Transl Med. 2020;10:91–106. https://doi.org/10.1002/ctm2.13.
45. Wang S, Tan J, Miao Y, Zhang Q. Mitochondrial dynamics, mitophagy, and mitochondria–endoplasmic reticulum contact sites crosstalk under hypoxia. Front Cell Dev Biol. 2022;10:848214. https://doi.org/10.3389/fcell.2022.848214.
46. Hu Y, Chen H, Zhang L, Lin X, Li X, Zhuang H, et al. The AMPK-MFN2 axis regulates MAM dynamics and autophagy induced by energy stresses. Autophagy. 2021;17:1142–56. https://doi.org/10.1080/15548627.2020.1749490.
47. Jacobi D, Liu S, Burkewitz K, Kory N, Knudsen NH, Alexander RK, et al. Hepatic Bmal1 regulates rhythmic mitochondrial dynamics and promotes metabolic fitness. Cell Metab. 2015;22:709–20. https://doi.org/10.1016/j.cmet.2015.08.006.
48. Li E, Li X, Huang J, Xu C, Liang Q, Ren K, et al. BMAL1 regulates mitochondrial fission and mitophagy through mitochondrial protein BNIP3 and is critical in the development of dilated cardiomyopathy. Protein Cell. 2020;11:661–79. https://doi.org/10.1007/s13238-020-00713-x.
49. Li CY, Wang W, Leung CH, Yang GJ, Chen J. KDM5 family as therapeutic targets in breast cancer: pathogenesis and therapeutic opportunities and challenges. Mol Cancer. 2024;23:109. https://doi.org/10.1186/s12943-024-02011-0.
50. Juhász KZ, Hajdú T, Kovács P, Vágó J, Matta C, Takács R. Hypoxic conditions modulate chondrogenesis through the circadian clock: the role of hypoxia-inducible factor-1α. Cells. 2024;13(6):512. https://doi.org/10.3390/cells13060512.
51. Yun Z, Maecker HL, Johnson RS, Giaccia AJ. Inhibition of *PPARγ2* gene expression by the HIF-1-regulated gene *DEC1/Stra13*: a mechanism for regulation of adipogenesis by hypoxia. Dev Cell. 2002;2:331–41. https://doi.org/10.1016/s1534-5807(02)00131-4.
52. Patke A, Young MW, Axelrod S. Molecular mechanisms and physiological importance of circadian rhythms. Nat Rev Mol Cell Biol. 2020;21:67–84. https://doi.org/10.1038/s41580-019-0179-2.
53. Wu Y, Tang D, Liu N, Xiong W, Huang H, Li Y, et al. Reciprocal regulation between the circadian clock and hypoxia signaling at the genome level in mammals. Cell Metab. 2017;25:73–85. https://doi.org/10.1016/j.cmet.2016.09.009.

Publisher's Note